

Range-Based Underwater Vehicle Localization in the Presence of Unknown Ocean Currents: Theory and Experiments

M. Bayat, N. Crasta, A. P. Aguiar, *Member, IEEE*, and A. M. Pascoal, *Member, IEEE*

Abstract—This paper addresses the problem of range-based Autonomous Underwater Vehicle (AUV) localization in the presence of unknown ocean currents. In the set-up adopted, the AUV is equipped with an Attitude and Heading Reference System (AHRS), a depth sensor, and an acoustic device that provides measurements of its distance to a set of stationary beacons. We consider the situation where the number of active beacons is not known in advance and may vary with time. The objective is to simultaneously localize the AUV and the beacons, that is, to find their positions underwater.

We start by deriving conditions under which it is possible to reconstruct the initial condition of the system under study. We consider the design model where the states evolve continuously with time but the range measurements are only available at discrete instants of time, possibly in a non-uniform manner. For trimming maneuvers that correspond to AUV trajectories with constant linear and angular velocities expressed in the body-frame, we show that if either the position of one of the beacons or the initial position of the AUV are known, then even without depth information the system is weakly observable (i.e., the set of states that are indistinguishable from a given initial configuration contains only a set of finite isolated points). If depth measurements are also available, then the system is observable even in the presence of unknown constant ocean currents.

Equipped with these results, we then propose a novel observer for simultaneous AUV and beacon localization. The mathematical set-up exploited borrows from minimum-energy estimation theory applied to continuous-time processes with discrete measurements, projection filters, and multiple-model estimation techniques. Convergence analysis of the resulting observer system yields conditions under which the estimation errors converge to a small neighborhood of the origin (whose size depends on the magnitude of the process and measurement noise). The results of field experiments with a robotic marine vehicle show the efficacy of the simultaneous AUV / multiple beacon localization system proposed.

Index Terms—Range-based underwater localization, autonomous underwater vehicles, observability analysis, minimum-energy observers.

I. INTRODUCTION

Autonomous underwater vehicles (AUVs) are steadily becoming the tool of choice for the execution of a vast

number of scientific and commercial missions at sea that include ocean data acquisition, remote sensing, and mapping of the spatial extent of pollutant spills, to name a few. Meeting these objectives requires that the AUVs be equipped with cost-effective, easy to install and use underwater navigation systems. Meeting this challenge may prove formidable, in view of the fact that conventional methods of vehicle localization that rely on GPS techniques cannot be used underwater, due to the high attenuation of electromagnetic signals.

The above problem can in principle be overcome by resorting to high-performance inertial navigation systems (INS). However, the costs of such systems may be prohibitive. Moreover, even with such high performance INS, drift is inevitable. Other possible solutions involve the use of acoustic based systems that rely on the measurements of the ranges between an AUV and a number of transponders in a baseline configuration or on the computation of range as well as bearing and elevation angles to a subsea transponder using an array of hydrophones that detect the incoming wave emitted by the transponder in response to a query by the AUV; see for example [1] for the description of localization techniques that include Ultra Short BaseLine (USBL), Long BaseLine (LBL), and GPS Intelligent Buoy (GIB) systems. In practice, acoustic localization systems are often affected by the presence of outliers, latency, and multi-path effects. In spite of this, however, acoustic based methods for underwater vehicle navigation are pervasive, and effective methodologies have been devised to deal with the aforementioned problems. More recently, an alternative technique for underwater vehicle localization has attracted considerable attention: range-only (also called single-beacon) based localization, whereby the position of an AUV is estimated by using discrete measurements of the ranges between the vehicle and a transponder fixed at a known location, while the AUV undergoes persistently exciting spatial maneuvers.

Previous work on single-beacon acoustic navigation can be traced back to [2], where a least-squares algorithm is proposed to compute the unknown initial position and constant speed of an AUV moving in the horizontal plane, subjected to an unknown constant current. The key concepts behind single-beacon navigation can also be found in the earlier work of [3], which describes a Synthetic Long BaseLine (SLBL) system based on the combination of dead-reckoning (DR) and acoustic range and/or range rate measurements from a single acoustic source, e.g., a transponder moored to the sea floor. Further relevant work can also be found in [4], where the authors

M. Bayat (corresponding author), N. Crasta, A. P. Aguiar, and A. M. Pascoal are with the Institute for Systems and Robotics (ISR), Instituto Superior Tecnico (IST), University of Lisbon, Portugal. {mbayat, ncrasta, pedro, antonio}@isr.ist.utl.pt. A. P. Aguiar is with Research Center for Systems and Technologies, Faculty of Engineering, University of Porto (FEUP), Portugal. pedro.aguiar@fe.up.pt. A. M. Pascoal is also an Adjunct Scientist with the National Institute of Oceanography (NIO) Goa, Dona Paula, 403-004, India.

describe an extended Kalman filter (EKF) for single-beacon navigation. In [5], by combining dead-reckoning data with measurements of the ranges between an underwater vehicle and a single beacon, taken at successive instants of time, a robust estimation algorithm is proposed for vehicle localization in the presence of unknown ocean currents. In [6], a method is described for precise post processed localization of a deep-diving AUV using only a set of acoustic ranges from a surface ship while the AUV executes a closed path under the ship. The approach is validated through experimental results with the Autosub 6000 AUV. For a concise and thorough presentation of previous work in the field and the description of a novel algorithm for single-beacon one-way-travel-time acoustic navigation for underwater vehicles, the reader is referred to [7], [8], and the references therein.

Some of the most recent solutions proposed for range-based localization borrow from the concept of Simultaneous Localization and Mapping (SLAM) that was first advanced in the field of mobile robots. The key idea of SLAM is to build a new map, or update an existing map of the environment, while at the same time localizing a robot within that map. Pioneering work in this area is described in [9], where a pure range-only sub-sea SLAM approach is described for AUV localization. The authors assume that the AUV is equipped with a conventional LBL transceiver that measures the acoustic times of flight (TOF) between the vehicle and a set of submerged transponders. Using only range data and no prior information other than the approximate water column depth, they present a methodology to compute both the transponder locations and the vehicle trajectories. See also [10], where a range-only simultaneous AUV and beacon localization system that assumes no prior knowledge of the beacons' locations and is robust against sensor noise and acoustic outliers is presented. More recently, in [11] the authors propose a range-only system for underwater vehicle localization that is based on a particle-filtering implementation of SLAM, coupled with a mixture-of-Gaussians representation of the posterior distribution of the beacons' positions.

No matter what particular algorithm is chosen for vehicle localization, a crucial and often forgotten issue is that of ascertaining the observability properties of the design model adopted. In the absence of observability the attempt to design a localization system will be destined to fail. For this reason, it is important to find conditions under which the design model of a range-based localization systems is observable. Examples of observability studies include the work described in [12], where a necessary and sufficient condition for local observability of a two-dimensional maneuvering target tracking system with range-only measurements is derived using estimation-theoretic methods. Historically, one of the first formal studies of observability of single-beacon AUV localization is described in [13], [14], where the authors use linearization techniques and classical tools of Linear Time Invariant (LTI) observability analysis. A different strategy is used in [15], [16] to study the observability of a range-based localization system by considering an equivalent augmented Linear Time Varying (LTV) and resorting to LTV system analysis tools. See also the approach in [16] for an interesting related study in the

discrete-time setting for uniform sampling set-up. Yet another approach is described in [17], where the authors study the problem of relative AUV localization using inter-vehicle range measurements by exploiting tools from nonlinear observability theory. The results obtained are validated experimentally in an equivalent single-beacon navigation scenario. In spite of substantial progress made in this area, however, work is still required to characterize explicitly the types of AUV trajectories that yield observability of range-based localization systems.

Motivated by the above considerations, the first part of this paper addresses key observability issues pertaining to the problem of range-based AUV localization using single and multiple fixed beacons, in the presence of constant unknown ocean currents. We consider explicitly the case where the positions of the beacons may be unknown, and thus require that they be localized as well. To this effect, we start by applying a coordinate transformation similar to the one presented in [18], implying a state augmentation that yields a state-affine system with algebraic constraints. We then establish, for the important case where the motion of the AUV is characterized by constant linear and angular velocities expressed in the body-frame (that is, trimming trajectories), conditions for which it is possible to reconstruct the initial state of the resulting system. The latter includes the position of the AUV as well as the positions of the beacons. In the analysis, we borrow from the nomenclature and the mathematical concepts of nonlinear system observability introduced by [19]. We show, under some reasonable practical conditions restricted to the assumption that the position of at least one of the beacons or the initial position of the AUV is known, that the localization system is at least weakly observable, meaning that the set of indistinguishable initial states is composed by a set of finite isolated points. By adding depth measurements or allowing the vehicle to undergo motion along the concatenation of at least two trimming trajectories, the resulting system becomes observable, in the sense that the set of indistinguishable points reduces to a singleton.

The key novel contributions that emerge from the first part of the work are the following: *i)* we derive conditions for the observability of the simultaneous AUV/beacon localization system in terms of AUV motion characteristics that are naturally expressed in the body frame and are therefore extremely easy to interpret, *ii)* we address the case where the location and number of the beacons may be unknown and vary over time, and *iii)* we assume explicitly that the state of the system under consideration evolves continuously in time but that the measurements occur at discrete times and the sampling time need not be constant (i.e., the measurement process is event-driven). Finally, *iv)* the above issues are tackled by assuming that there may be unknown but constant currents. Previous related work on the issue of observability in the absence of currents and assuming continuous time measurements can be found in [20].

The second part of the paper addresses the problem of range-based localization system design. We exploit the observability properties derived in the first part of the paper and use the concepts of minimum-energy estimation, projection filters, and multiple-model estimation techniques, to derive a novel

observer that solves the AUV localization problem using relative range measurements to stationary beacons, the locations of which may also be unknown. In contrast to a number of results described in the literature, we give conditions under which the AUV and beacon estimation errors converge to a small neighborhood of zero (whose size depends on the magnitude of the process/measurement noise). The rationale behind the use of the techniques adopted stems from the following facts:

- i) we resort to minimum-energy observers in a deterministic setting because, as will become clear later, for the localization problem at hand it is not natural to assume that the state and observation noise are stochastic processes with Gaussian distributions. This is in striking contrast to the assumptions that are at the root of Kalman filter designs in a stochastic setting. We remind the reader that a minimum-energy observer is an optimal filter that produces an estimate of the state of a system that is most compatible with the system dynamics and measured outputs for the lowest possible energy of the state and observation noise signals [21]. For linear systems, minimum-energy observers yield a structure akin to that of Kalman filters, albeit in a fully deterministic framework. See for example in [18] the derivation of a minimum-energy estimator for linear dynamic systems with perspective outputs. The deterministic set-up adopted affords us an expedite manner to assess the convergence properties of the proposed estimator in terms of bounds on the magnitude of the process and measurement noise.
- ii) the state-affine design model that we develop has the interesting property that the state must satisfy a set of quadratic constraints. To address these constraints explicitly, we exploit the techniques proposed in [21] to solve the problem of minimum-energy state estimation for systems with perspective outputs and state constraints. They lead naturally to a so-called projection filter that improves significantly the performance of the proposed observer;
- iii) localizing the beacons arises naturally from the fact that we are also interested in estimating the location of the beacons whose number and positions may be unknown; and finally,
- iv) the multiple-model approach adopted allows us to address explicitly the fact that, according to the observability results obtained, there may be distinct AUV trajectories (generated by the same input) corresponding to multiple, isolated initial conditions that will yield the same output time histories.

The efficacy of the proposed observer structure is validated through real-world field experiments using the MEDUSA-class of autonomous marine robotic vehicles equipped with ranging devices. In the experiment, one of the vehicles plays the role of an AUV while the other two serve as proxies for underwater beacons.

The paper is organized as follows: Section II derives the model underlying the design of a range-based localization system with single or multiple beacons. The observability analysis of the proposed design model is done in Section III.

Section IV derives the observer that is used to estimate the states of the system and discusses its convergence properties in Section V. Section VI describes experimental results with a set of marine vehicles that show the efficacy of the nonlinear observer and illustrate the implications of the observability conditions derived. Concluding remarks are given in Section VII. *All the proofs of the theorems in Section III are presented in the Appendix.*

II. PROCESS MODEL

This section introduces the model adopted to design an AUV localization system that relies on the computation of the ranges between the vehicle and one or more underwater beacons, the location of which may be unknown. The objective is to compute in real time an estimate of the position of the AUV and simultaneously construct a map composed by the estimates of the locations of the beacons. We consider that the AUV motion is subjected to the influence of unknown but constant ocean currents. In what follows, we introduce two coordinate frames: an Earth-fixed or inertial coordinate frame $\{\mathcal{I}\}$ and a body-fixed coordinate frame $\{\mathcal{B}\}$ that is attached to the AUV and moves with it. We let $({}^{\mathcal{I}}\mathbf{p}_{\mathcal{B}}, {}^{\mathcal{I}}\mathcal{R}) \in \mathbb{R}^3 \times \text{SO}(3)$ be the configuration of frame $\{\mathcal{B}\}$ with respect to $\{\mathcal{I}\}$, where ${}^{\mathcal{I}}\mathbf{p}_{\mathcal{B}}$ is the position of the AUV in frame $\{\mathcal{I}\}$ and ${}^{\mathcal{I}}\mathcal{R}$ is the rotation matrix from $\{\mathcal{B}\}$ to $\{\mathcal{I}\}$. We denote by $\text{SO}(3)$ the group of special orthogonal matrices in three dimensional space. With this notation, the kinematic equations of motion of the AUV can be written as

$${}^{\mathcal{I}}\dot{\mathbf{p}}_{\mathcal{B}} = {}^{\mathcal{I}}\mathcal{R}\boldsymbol{\nu} + {}^{\mathcal{I}}\boldsymbol{\nu}_c \quad (1)$$

$${}^{\mathcal{I}}\dot{\mathcal{R}} = {}^{\mathcal{I}}\mathcal{R}S(\boldsymbol{\omega}) \quad (2)$$

$${}^{\mathcal{I}}\dot{\boldsymbol{\nu}}_c = \mathbf{0} \quad (3)$$

where $\boldsymbol{\nu}, \boldsymbol{\omega}: [0, \infty) \rightarrow \mathbb{R}^3$ denote the body-fixed linear and angular velocities of the AUV respectively, relative to $\{\mathcal{I}\}$, expressed in $\{\mathcal{B}\}$, ${}^{\mathcal{I}}\boldsymbol{\nu}_c \in \mathbb{R}^3$ is an unknown constant ocean current in $\{\mathcal{I}\}$ and, for every $\mathbf{a} \in \mathbb{R}^3$,

$$S(\mathbf{a}) := \begin{bmatrix} 0 & -a_3 & a_2 \\ a_3 & 0 & -a_1 \\ -a_2 & a_1 & 0 \end{bmatrix}$$

is the skew-symmetric matrix representing the linear map $\mathbf{a} \mapsto \mathbf{a} \times \mathbf{b}$, $\mathbf{b} \in \mathbb{R}^3$, where “ \times ” is the standard cross product in \mathbb{R}^3 .

In what follows we will treat the linear and angular velocities $\boldsymbol{\nu}$ and $\boldsymbol{\omega}$ as inputs to the system (1)-(3) and use the Euler angle vector $\boldsymbol{\eta} = [\phi, \theta, \psi] \in [0, 2\pi) \times (-\frac{\pi}{2}, \frac{\pi}{2}) \times [0, 2\pi)$ to parametrize the rotation matrix ${}^{\mathcal{I}}\mathcal{R}$, locally. For simplicity we denote $c\theta := \cos \theta$ and $s\theta := \sin \theta$. Let $n \in \mathbb{N}$ be the number of stationary beacons q_i located at ${}^{\mathcal{I}}\mathbf{q}_i = [x_i, y_i, z_i]' \in \mathbb{R}^3$, $i \in \{1, 2, \dots, n\}$ which we assume are not known, with the exception of their depth coordinates z_i . Clearly,

$${}^{\mathcal{I}}\dot{\mathbf{q}}_i = \mathbf{0}. \quad (4)$$

For each $i \in \{1, 2, \dots, n\}$, let $r_i(t)$ be the acoustic-based measurement of the range between the AUV and the i^{th} beacon, acquired at time $t \geq 0$. Assuming that the depth z_0

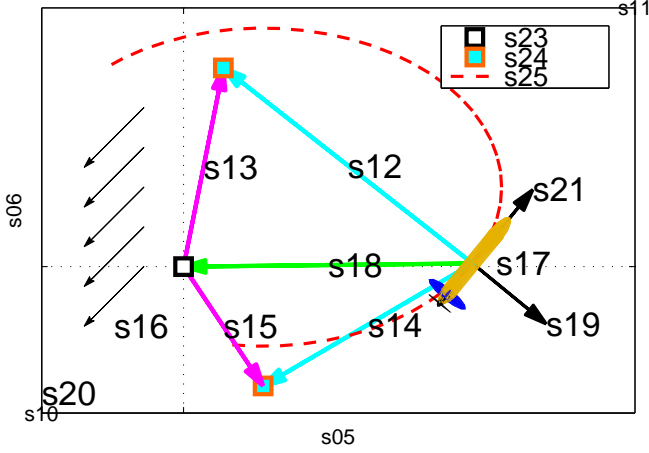


Fig. 1. Illustration of representative state vectors in 2D space.

of the AUV can be measured, the measurement/output model that we adopt can be written as

$$r_i = \|\mathcal{I} \mathbf{q}_i - \mathcal{I} \mathbf{p}_B\| \quad (5)$$

$$z_i = \mathbf{e}'_z \mathcal{I} \mathbf{q}_i \quad (6)$$

$$z_0 = \mathbf{e}'_z \mathcal{I} \mathbf{p}_B \quad (7)$$

where $\mathbf{e}_x = [1, 0, 0]'$, $\mathbf{e}_y = [0, 1, 0]'$, $\mathbf{e}_z = [0, 0, 1]'$.

Equations (1)-(7) represent the nonlinear continuous model of the multiple beacon-AUV localization problem that we address in this paper. In the sequel, for observability analysis purposes, we will construct a state-affine system and derive conditions under which this new system is *equivalent* to (1)-(7), in the sense that there is a one-to-one correspondence between the state trajectories of the original nonlinear system and the newly constructed one. We remark that the strategy adopted to obtain the equivalent state-affine system does not follow the ones described in [22], [23], but is instead tailored to our specific application. The key ideas exploited are to express the positions of the beacons \mathbf{q}_i in the body frame $\{\mathcal{B}\}$ and to introduce a *virtual* beacon, \mathbf{q}_0 , located at an arbitrary point that we take as the origin of the inertial frame $\{\mathcal{I}\}$ (see Fig. 1). Following this strategy and exploiting some of the concepts presented in [18] we define

$$\mathcal{B} \mathbf{p}_i = \mathcal{I} \mathcal{R}' \mathcal{I} \mathbf{q}_i - \mathcal{I} \mathcal{R}' \mathcal{I} \mathbf{p}_B \quad i \in \{0, 1, \dots, n\}, \quad (8)$$

as the vector directed from the vehicle to beacon \mathbf{q}_i , expressed in $\{\mathcal{B}\}$. From (1), (2), and (4) it follows that

$$\begin{aligned} \mathcal{B} \dot{\mathbf{p}}_i &= \mathcal{I} \mathcal{R}' (\mathcal{I} \dot{\mathbf{q}}_i - \mathcal{I} \dot{\mathbf{p}}_B) + \mathcal{I} \mathcal{R}' \mathcal{I} \dot{\mathbf{q}}_i - \mathcal{I} \mathcal{R}' \mathcal{I} \dot{\mathbf{p}}_B \\ &= -S(\omega) \mathcal{B} \mathbf{q}_i - \boldsymbol{\nu} - \mathcal{B} \boldsymbol{\nu}_c \end{aligned}$$

Using (2) and the equalities $\mathcal{B} \boldsymbol{\nu}_c = \mathcal{I} \mathcal{R}' \mathcal{I} \boldsymbol{\nu}_c$ and $\mathcal{B} \mathbf{q}_i = \mathcal{I} \mathcal{R}' \mathcal{I} \mathbf{q}_i$ it can be verified that

$$\mathcal{B} \dot{\boldsymbol{\nu}}_c = -S(\omega) \mathcal{B} \boldsymbol{\nu}_c, \quad \mathcal{B} \dot{\mathbf{q}}_i = -S(\omega) \mathcal{B} \mathbf{q}_i.$$

Furthermore, from (8) and the fact that $\mathcal{B} \mathbf{q}_i = \mathcal{B} \mathbf{p}_i - \mathcal{B} \mathbf{p}_0$ the range measurement equation (5) can be written as

$$r_i = \|\mathcal{I} \mathbf{q}_i - \mathcal{I} \mathbf{p}_B\| = \|\mathcal{I} \mathcal{R}' \mathcal{B} \mathbf{q}_i\| = \|\mathcal{B} \mathbf{q}_i + \mathcal{B} \mathbf{p}_0\|$$

where the last equality follows from the fact that any rotation matrix is orthogonal.

To make the output equation (5) linear in the state variables we rewrite it as $r_i = \chi_i$, with $\chi_i := \|\mathcal{B} \mathbf{q}_i + \mathcal{B} \mathbf{p}_0\|$ viewed as a new extra state variable. Straightforward computations yield

$$\dot{\chi}_i = -(\boldsymbol{\nu}' (\mathcal{B} \mathbf{q}_i + \mathcal{B} \mathbf{p}_0) + \mathcal{B} \boldsymbol{\nu}'_c (\mathcal{B} \mathbf{q}_i + \mathcal{B} \mathbf{p}_0)) / r_i. \quad (9)$$

Notice that (9) is not valid when $r_i = 0$, which corresponds to the particular case where the position of the AUV coincides with the location of the i^{th} beacon. To avoid this singularity (in particular at the observer design stage), one possible simple solution is to add a small term $\epsilon > 0$ to r_i in (9). This term can be a function of r_i , and must be defined so as to be nonzero when $r_i = 0$. From a practical point of view this issue can be avoided by preventing the vehicle's position to coincide with one of the positions of the beacons. For example, by positioning the latter at depths different from those where the AUV is expected to operate. Notice also that (9) contains nonlinear terms such as the products of state variables. To deal with this fact, we introduce an additional set of $n+1$ state variables. Define $\chi_c := \mathcal{B} \boldsymbol{\nu}'_c \mathcal{B} \boldsymbol{\nu}_c$ and, for each $i \in \{1, \dots, n\}$, let $\chi_{c_i} := \mathcal{B} \boldsymbol{\nu}'_c (\mathcal{B} \mathbf{q}_i + \mathcal{B} \mathbf{p}_0)$. Straightforward computations show that

$$\begin{aligned} \dot{\chi}_i &= -(\boldsymbol{\nu}' (\mathcal{B} \mathbf{q}_i + \mathcal{B} \mathbf{p}_0) + \chi_{c_i}) / r_i, \\ \dot{\chi}_{c_i} &= \mathcal{B} \boldsymbol{\nu}'_c S(\omega) \mathcal{B} \mathbf{p}_0 - \mathcal{B} \boldsymbol{\nu}'_c (S(\omega) \mathcal{B} \mathbf{p}_0 + \boldsymbol{\nu} + \mathcal{B} \boldsymbol{\nu}_c) \\ &\quad + \mathcal{B} \boldsymbol{\nu}'_c S(\omega) \mathcal{B} \mathbf{q}_i - \mathcal{B} \boldsymbol{\nu}'_c S(\omega) \mathcal{B} \mathbf{q}_i = -\boldsymbol{\nu}' \mathcal{B} \boldsymbol{\nu}_c - \chi_{c_i}, \\ \dot{\chi}_c &= \mathcal{B} \boldsymbol{\nu}'_c S(\omega) \mathcal{B} \boldsymbol{\nu}_c - \mathcal{B} \boldsymbol{\nu}'_c S(\omega) \mathcal{B} \boldsymbol{\nu}_c = 0. \end{aligned}$$

Using the equalities $\mathcal{I} \mathbf{q}_i = \mathcal{I} \mathcal{R}' \mathcal{B} \mathbf{q}_i$ and $\mathcal{I} \mathbf{p}_B = -\mathcal{I} \mathcal{R}' \mathcal{B} \mathbf{p}_0$, the output equations (6) and (7) can be written as

$$z_i = \mathbf{e}'_z \mathcal{I} \mathcal{R}' \mathcal{B} \mathbf{q}_i, \quad z_0 = -\mathbf{e}'_z \mathcal{I} \mathcal{R}' \mathcal{B} \mathbf{p}_0.$$

Putting together the above equations, we obtain a state-affine system with state vector $\mathbf{x} \in \mathbb{R}^{5n+7}$, input vector $\mathbf{u} \in \mathbb{R}^9$, and output vector $\mathbf{y} \in \mathbb{R}^{2n+1}$, described by

$$\begin{cases} \dot{\mathbf{x}}(t) = \mathbf{A}_{\mathbf{u}, \mathbf{y}}(t) \mathbf{x}(t) + \mathbf{b}_{\mathbf{u}}(t) \\ \mathbf{y}(t) = \mathbf{C}_{\mathbf{u}}(t) \mathbf{x}(t) \end{cases} \quad (10)$$

where

$$\begin{aligned} \mathbf{x} &:= [\mathcal{B} \mathbf{p}'_0, [\mathcal{B} \mathbf{q}'_1 \dots \mathcal{B} \mathbf{q}'_n], \mathcal{B} \boldsymbol{\nu}'_c, \chi_c, [\chi_{c_1} \dots \chi_{c_n}], [\chi_1 \dots \chi_n]]', \\ \mathbf{u} &:= [\boldsymbol{\nu}' \quad \boldsymbol{\omega}' \quad \boldsymbol{\eta}'']', \quad \mathbf{y} := [[r_1 \dots r_n], z_0, [z_1 \dots z_n]]', \\ \mathbf{s} &:= [\frac{1}{r_1} \quad \frac{1}{r_2} \quad \dots \quad \frac{1}{r_n}]', \quad \Omega := S(\omega), \\ \mathbf{A}_{\mathbf{u}, \mathbf{y}} &:= - \begin{bmatrix} \Omega & \mathbf{0} & \mathbf{I}_3 & \mathbf{0} & \mathbf{0} & \mathbf{0} \\ \mathbf{0} & \mathbf{I}_n \otimes \Omega & \mathbf{0} & \mathbf{0} & \mathbf{0} & \mathbf{0} \\ \mathbf{0} & \mathbf{0} & \Omega & \mathbf{0} & \mathbf{0} & \mathbf{0} \\ \mathbf{0} & \mathbf{0} & \mathbf{0} & \mathbf{0} & \mathbf{0} & \mathbf{0} \\ \mathbf{0} & \mathbf{0} & \mathbf{0} & \mathbf{0} & \mathbf{0} & \mathbf{0} \\ \mathbf{s} \otimes \boldsymbol{\nu}' & \text{diag}(\mathbf{s}) \otimes \boldsymbol{\nu}' & \mathbf{0} & \mathbf{0} & \text{diag}(\mathbf{s}) & \mathbf{0} \end{bmatrix}, \quad \mathbf{b}_{\mathbf{u}} := \begin{bmatrix} -\boldsymbol{\nu} \\ \mathbf{0} \\ \mathbf{0} \\ \mathbf{0} \\ \mathbf{0} \\ \mathbf{0} \end{bmatrix}, \\ \mathbf{C}_{\mathbf{u}} &:= \begin{bmatrix} \mathbf{0} & \mathbf{0} & \mathbf{0} & \mathbf{0} & \mathbf{0} & \mathbf{I}_n \\ -\mathbf{e}'_z \mathcal{I} \mathcal{R}'(\boldsymbol{\eta}) & \mathbf{0} & \mathbf{0} & \mathbf{0} & \mathbf{0} & \mathbf{0} \\ \mathbf{0} & \mathbf{I}_n \otimes (\mathbf{e}'_z \mathcal{I} \mathcal{R}') & \mathbf{0} & \mathbf{0} & \mathbf{0} & \mathbf{0} \end{bmatrix} \end{aligned}$$

that satisfies the following quadratic constraints for each $i \in \{1, 2, \dots, n\}$:

$$\chi_i^2 = \|\mathcal{B} \mathbf{q}_i + \mathcal{B} \mathbf{p}_0\|^2, \quad (11)$$

$$\chi_c = \|\mathcal{B} \boldsymbol{\nu}_c\|^2, \quad (12)$$

$$\chi_{c_i} = \mathcal{B} \boldsymbol{\nu}'_c (\mathcal{B} \mathbf{q}_i + \mathcal{B} \mathbf{p}_0). \quad (13)$$

In the above model, we have used the following notation: given $M_1, M_2 \in \mathbb{R}^{m_i \times n_i}$ and $\mathbf{v} \in \mathbb{R}^n$, we denote by $M_1 \otimes M_2 \in \mathbb{R}^{m_1 n_1 \times m_2 n_2}$ the Kronecker product of M_1 by M_2 and by $\text{diag}(\mathbf{v})$ the diagonal $n \times n$ matrix with its main diagonal given by \mathbf{v} . Moreover, $\mathbf{0}$, $\mathbf{1}_n$, and I_n denote a zero matrix of appropriate dimension, a column vector of ones with length n , and the identity matrix of size n , respectively.

Note that for any trajectory in the state-space of the original system (1)-(3) there is a unique corresponding trajectory in the augmented state-space of system (10). Conversely, combining the quadratic constraints (11)-(13) with the state-affine system (10) guarantees that every trajectory of (10) has a corresponding state-space trajectory in (1)-(3). Once an equivalent state-affine system is obtained, one can resort to powerful tools of linear systems theory for observability analysis.

An important problem that needs to be addressed explicitly is the fact that due to practical limitations, range/depth measurements are only available at discrete instants of time. This has direct impact on the observability of the underlying model as well as on the performance of a corresponding observer. Furthermore, the observations may not even be periodic due to the fact that the times taken by acoustic waves to travel between the beacons and the AUV will depend on their relative positions. To accommodate these issues, we adopt the following model with continuous-time state dynamics and discrete observations:

$$\begin{cases} \dot{\mathbf{x}}(t) = A_{\mathbf{u}, \mathbf{y}}(t)\mathbf{x}(t) + \mathbf{b}_{\mathbf{u}}(t) \\ \mathbf{y}(t_k) = C_{\mathbf{u}}(t_k)\mathbf{x}(t_k) \end{cases} \quad (14)$$

where the possible non-uniform times $t_k, k \in \{0, 1, 2, \dots\}$, are the instants at which range/depth measurements are acquired on board the AUV.

III. OBSERVABILITY ANALYSIS

This section addresses the observability of the model introduced in section II. Specifically, given the dynamical system (14) with unknown initial condition $\mathbf{x}(t_0) = \mathbf{x}_0$, subject to (11)-(13), the objective is to determine conditions under which it will be possible to compute \mathbf{x}_0 from the knowledge of the input/output time histories $\{\mathbf{u}(t), t \in [t_0, t_f], \mathbf{y}(t_k), t_k \in [t_0, t_f]\}$ for some $t_f > t_0$.

To set the stage for a formal discussion of observability, we first introduce the following definitions adopted from [19], [24]. Notice however that in this paper, for observability analysis purposes, we will not adopt the observability conditions derived in [19] for general nonlinear systems. Instead, we will derive specific conditions for the system under study that are simple to characterize in terms of the type of motion imparted to the AUV.

Definition 1. *Given the system (14) and a time interval $[t_0, t_f]$, two initial conditions $\mathbf{z}, \tilde{\mathbf{z}}$ are said to be indistinguishable on $[t_0, t_f]$ if the output-time histories $\{\mathbf{y}(t_k), t_k \in [t_0, t_f]\}$, resulting from all admissible input time series $\{\mathbf{u}(t), t \in [t_0, t_f]\}$ and satisfying the initial conditions $\mathbf{x}(t_0) = \mathbf{z}$ and $\mathbf{x}(t_0) = \tilde{\mathbf{z}}$ are identical. For every \mathbf{z} , $\mathcal{I}(\mathbf{z})$ denotes the set of all initial conditions that are indistinguishable from \mathbf{z} on $[t_0, t_f]$.*

Definition 2. *The system (14) is observable at \mathbf{z} on $[t_0, t_f]$ if $\mathcal{I}(\mathbf{z}) = \{\mathbf{z}\}$, and it is observable on $[t_0, t_f]$ if $\mathcal{I}(\mathbf{z}) = \{\mathbf{z}\}$ for every \mathbf{z} .*

Definition 3. *The system (14) is weakly observable at \mathbf{z} on $[t_0, t_f]$ if \mathbf{z} is an isolated point of $\mathcal{I}(\mathbf{z})$ and it is weakly observable on $[t_0, t_f]$ if it is weakly observable for every \mathbf{z} .*

Notice that weak observability at a point \mathbf{z} does not imply that every input from the class \mathcal{U}_{ad} of admissible inputs will distinguish \mathbf{z} from any other state in a small neighborhood of \mathbf{z} . Different inputs may be required to distinguish \mathbf{z} from other states in that neighborhood. For this reason, the notion of observability defined above, even though elegant, may not be entirely satisfactory in a number of applications. Interestingly enough, in some engineering problems dealing with autonomous vehicles there exist reduced classes $\mathcal{U}_c \subseteq \mathcal{U}_{ad}$ of admissible input signals named \mathbf{u}^* , sufficiently general to yield maneuvers of interest in a wide range of applications, and yet restricted in the sense that they can be easily parametrized in terms of a small number of parameters with a strong physical interpretation. Such is the case with AUVs when they undergo motion along trimming trajectories (generated by holding the input actuators fixed) that are easily parametrized by total speed, yaw rate, and flight path angle and correspond to helices in 3D space that may degenerate into circumferences and straight lines [25]. In these cases, it is of interest to a practitioner to ascertain the observability properties of a given system for a reduced class of inputs \mathcal{U}_c , rather than allowing for all inputs that are physically admissible. Motivated by these considerations, we introduce a weaker notion of observability originally proposed in [26], that, as we shall see, will allow for the derivation of observability condition for the localization system studied in this paper that are easy to interpret physically.

Definition 4. *Given the system (14) and a time interval $[t_0, t_f]$, two initial conditions $\mathbf{z}, \tilde{\mathbf{z}}$ are said to be \mathbf{u}^* -indistinguishable on $[t_0, t_f]$ if the output-time histories $\{\mathbf{y}(t_k), t_k \in [t_0, t_f]\}$, for an input time series $\{\mathbf{u}^*(t) \in \mathcal{U}_c, t \in [t_0, t_f]\}$ and satisfying the initial conditions $\mathbf{x}(t_0) = \mathbf{z}$ and $\mathbf{x}(t_0) = \tilde{\mathbf{z}}$ are identical. For every \mathbf{z} , $\mathcal{I}^{\mathbf{u}^*}(\mathbf{z})$ denotes the set of all initial conditions that are \mathbf{u}^* -indistinguishable from \mathbf{z} on $[t_0, t_f]$.*

Definition 5. *Given $\mathbf{u}^* \in \mathcal{U}_c$ and a time interval $[t_0, t_f]$, the system (14) is \mathbf{u}^* -observable at \mathbf{z} on $[t_0, t_f]$ if $\mathcal{I}^{\mathbf{u}^*}(\mathbf{z}) = \{\mathbf{z}\}$, and is \mathbf{u}^* -observable on $[t_0, t_f]$ if $\mathcal{I}^{\mathbf{u}^*}(\mathbf{z}) = \{\mathbf{z}\}$ for every \mathbf{z} .*

Definition 6. *Given $\mathbf{u}^* \in \mathcal{U}_c$ and a time interval $[t_0, t_f]$, the system (14) is \mathbf{u}^* -weakly observable at \mathbf{z} on $[t_0, t_f]$ if \mathbf{z} is an isolated point of $\mathcal{I}^{\mathbf{u}^*}(\mathbf{z})$ and is \mathbf{u}^* -weakly observable on $[t_0, t_f]$ if it is \mathbf{u}^* -weakly observable for every \mathbf{z} .*

Note that observability implies weak observability and \mathbf{u}^* -observability implies \mathbf{u}^* -weak observability. Throughout the paper we will use the weaker notions of observability. To simplify the terminology, we shall often abbreviate the nomenclature of \mathbf{u}^* -indistinguishable, \mathbf{u}^* -observable, and \mathbf{u}^* -weakly observable to indistinguishable, observable, and weakly observable, respectively.

We now define formally the class of admissible inputs $\mathbf{u} \in \mathcal{U}_c$ that we consider for the system described by (14). To this effect, as explained before, we restrict ourselves to AUV trimming (also called equilibrium or steady state) trajectories. Straightforward computations similar to those in [25] done for the case of aircraft show that at trimming

$$\boldsymbol{\omega}_e = \dot{\psi}_e [-s\theta_e \quad s\phi_e c\theta_e \quad c\phi_e c\theta_e]' = \dot{\psi}_e \mathcal{I}_B \mathcal{R}'(\boldsymbol{\eta}_e) \mathbf{e}_z, \quad (15)$$

where the subscript “e” denotes the value of a variable at steady state and $\phi(t) = \phi_e$, $\theta(t) = \theta_e$, and $\dot{\psi}_e$ are the values of roll angle, pitch angle, and yaw rate respectively, at steady state.

For clarity of exposition, the observability analysis will be first carried out for the case of one beacon only, that is, $n = 1$. We will also work with the states χ_1^2 and r_1^2 (squared range output) instead of χ_1 and r_1 , respectively. With these assumptions, (14) yields

$$\begin{cases} \dot{\mathbf{x}}(t) = \mathbf{A}_u(t)\mathbf{x}(t) + \mathbf{b}_u(t) \\ \mathbf{y}(t_k) = \mathbf{C}_u(t_k)\mathbf{x}(t_k) \end{cases} \quad (16)$$

where $\mathbf{x} := [\mathcal{B}p_0' \quad \mathcal{B}q_1' \quad \mathcal{B}v_c' \quad \chi_e \quad \chi_{c1} \quad \chi_1^2]'$, $\mathbf{y} := [r_1^2 \quad z_0 \quad z_1]'$, $\mathbf{u} := [\nu_e' \quad \omega_e' \quad \phi_e \quad \theta_e']'$, and

$$\mathbf{A}_u := - \begin{bmatrix} \Omega_e & 0 & I_3 & 0 & 0 & 0 \\ 0 & \Omega_e & 0 & 0 & 0 & 0 \\ 0 & 0 & \Omega_e & 0 & 0 & 0 \\ 0 & 0 & 0 & 0 & 0 & 0 \\ 0 & 0 & \nu_e' & 1 & 0 & 0 \\ 2\nu_e' & 2\nu_e' & 0 & 0 & 2 & 0 \end{bmatrix}, \mathbf{b}_u := \begin{bmatrix} -\nu_e \\ 0 \\ 0 \\ 0 \\ 0 \\ 0 \end{bmatrix},$$

$$\mathbf{C}_u := \begin{bmatrix} 0 & 0 & 0 & 0 & 0 & 0 & 0 & 1 \\ s\theta_e & -s\phi_e c\theta_e & -c\phi_e c\theta_e & 0 & 0 & 0 & 0 & 0 \\ 0 & 0 & 0 & -s\theta_e & s\phi_e c\theta_e & c\phi_e c\theta_e & 0 & 0 \end{bmatrix}.$$

At this point it is important to note that working with the square of the ranges rather than the ranges themselves does not change the observability results. Suppose for example that (16) is \mathbf{u}^* -observable for a given input \mathbf{u}^* , in the sense that for every pair of distinct initial conditions $(\mathbf{x}_0, \mathbf{z}_0)$ there exists a time interval $t \in [t^*, t_f]$, $t^* \geq 0$ such that the corresponding squared range outputs are different, that is, $y(t; \mathbf{u}^*, \mathbf{x}_0) := r_1^2(t; \mathbf{u}^*, \mathbf{x}_0) \neq y(t; \mathbf{u}^*, \mathbf{z}_0) := r_1^2(t; \mathbf{u}^*, \mathbf{z}_0)$. Then, it also follows that $r_1(t; \mathbf{u}^*, \mathbf{x}_0) \neq r_1(t; \mathbf{u}^*, \mathbf{z}_0)$, which implies that the initial conditions $(\mathbf{x}_0, \mathbf{z}_0)$ for the original system (using ranges) will produce different outputs. The converse implication holds as well.

In what follows, for simplicity of analysis, we will rewrite equations (16) by considering the so-called *flow frame* $\{\mathcal{F}\}$ (also called wind frame in aerodynamics), instead of the body fixed frame $\{\mathcal{B}\}$. With this change of reference frames, the total velocity vector at trimming is aligned with the x -axis of $\{\mathcal{F}\}$, that is, $\boldsymbol{\nu}_e = [\nu_e, 0, 0]'$. As is well known, the transformation from flow frame to body fixed frame is done using a rotation matrix parametrized by the angles of attack and side-slip, which are constant during a trimming maneuver. Expressed in the flow frame, the body angular velocity is also constant at trimming. Therefore, after straightforward computations it can be concluded that the single-beacon system using the linear velocity $\boldsymbol{\nu}$ and the angular velocity $\boldsymbol{\omega}$ expressed in the flow frame take the same form as (16), where in this case the orientation parametrized by $\boldsymbol{\eta}$ is with respect to $\{\mathcal{F}\}$. Throughout the paper, for simplicity

of exposition and to avoid changing the notation, we continue to adopt the model defined by (16), with the understanding that the variables are expressed in flow frame.

Returning to the observability problem, one immediate result is that, unless there is an *anchor* which relates relative localization with global (inertial) position, the system (16) is not observable. This is due to the fact that range is a relative measurement. To deal with this problem that arises in any simultaneous localization and mapping approach, the idea is to use a priori knowledge of the position of one of the beacons/AUV and estimate the other unknown ones. For instance, one practical scenario is to consider that the initial position of the AUV is known, which is feasible if the AUV starts from the surface with GPS. Another approach is to consider that the location of one of the beacons is known. In the sequel we consider the case where the initial condition of the beacon $\mathcal{B}q_1(0)$ is known. Later on we will investigate the dual case where the initial location of AUV $\mathcal{B}p_0(0)$ is known.

Given $\mathbf{x}_0 \in \mathbb{R}^{12}$, let $\mathcal{I}_r(\mathbf{x}_0)$ denote the set of indistinguishable initial conditions from \mathbf{x}_0 for the system (16) with range-only measurements. The main result of this section is stated in the next theorem, which characterizes $\mathcal{I}_r(\cdot)$ under some conditions.

Theorem 1. *Consider the (16) with range-only measurement, that is, $\mathbf{C}_u = [\mathbf{0}, 1]$ subject to constraints (11)-(13). Suppose that $\boldsymbol{\omega}_e = [\omega_{e_x}, \omega_{e_y}, \omega_{e_z}]' \in \mathbb{R}^3$ satisfies*

$$\|\boldsymbol{\omega}_e\| > \|\omega_{e_x}\|, \quad (17)$$

and the number of available samples of measurements on $[t_0, t_f]$ is at least 7 (that is $n_r \geq 7$). Moreover, let the inter-arrival times, $t_{k+1} - t_k$, be strictly positive. Then, for every $\mathbf{x}_0 \in \mathbb{R}^{12}$ and almost all inter-arrival times, the set of all initial conditions that are indistinguishable from \mathbf{x}_0 on $[t_0, t_f]$ is given by

$$\mathcal{I}_r(\mathbf{x}_0) = \left\{ \mathbf{x}_0, \mathbf{x}_0 + \frac{2}{\omega_e' \omega_e} \begin{bmatrix} -\omega_e \omega_e' (\mathcal{B}p_0(0) + \mathcal{B}q_1(0)) \\ \mathbf{0} \\ -\omega_e \omega_e' (\mathcal{B}v_c(0) + \boldsymbol{\nu}_e) \\ 2\nu_e' \omega_e \omega_e' (\mathcal{B}v_c(0) + \boldsymbol{\nu}_e) \\ \nu_e' \omega_e \omega_e' (\mathcal{B}p_0(0) + \mathcal{B}q_1(0)) \\ 0 \end{bmatrix} \right\}. \quad (18)$$

Further, in this case, the system (16) subject to constraints (11)-(13) is weakly observable on $[t_0, t_f]$. Consider now the degenerate case where the inter-arrival times are uniform, that is, $t_{k+1} - t_k = T$ for all $t_k \in [t_0, t_f]$. Then, for all inter-arrival times except for the zero measure set

$$\left\{ t_k \mid t_{k+1} - t_k = \kappa\pi \|\boldsymbol{\omega}_e\|^{-1}, t_k \in [t_0, t_f], \kappa \in \mathbb{N}^+ \right\} \quad (19)$$

the set of all initial conditions that are indistinguishable from a given initial condition $\mathbf{x}_0 \in \mathbb{R}^{12}$ on $[t_0, t_f]$ is given by (18).

The above theorem allows for a simple geometrical interpretation of the non-trivial point in $\mathcal{I}_r(\mathbf{x}_0)$. This stems from the fact that the components of the non-trivial point in $\mathcal{I}_r(\mathbf{x}_0)$ given by the AUV position and the ocean current velocity can

be written as

$$\begin{aligned}\check{\mathcal{B}}\mathbf{p}_0(0) &:= (I_3 - 2\|\boldsymbol{\omega}_e\|^{-2}\boldsymbol{\omega}_e\boldsymbol{\omega}'_e)(\mathcal{B}\mathbf{p}_0(0) + \mathcal{B}\mathbf{q}_1(0)) - \mathcal{B}\mathbf{q}_1(0), \\ \check{\mathcal{B}}\boldsymbol{\nu}_c(0) &:= (I_3 - 2\|\boldsymbol{\omega}_e\|^{-2}\boldsymbol{\omega}_e\boldsymbol{\omega}'_e)(\mathcal{B}\boldsymbol{\nu}_c(0) + \boldsymbol{\nu}_e) - \boldsymbol{\nu}_e.\end{aligned}$$

Note that from the Rodrigues' rotation formula [27], it follows that $I_3 - 2\|\boldsymbol{\omega}_e\|^{-2}\boldsymbol{\omega}_e\boldsymbol{\omega}'_e = -R(\pi, \boldsymbol{\omega}_e/\|\boldsymbol{\omega}_e\|)$. Geometrically, this represents the rotation of $-(\mathcal{B}\mathbf{p}_0(0) + \mathcal{B}\mathbf{q}_1(0))$ about the $\boldsymbol{\omega}_e$ axis by π . In other words, $\check{\mathcal{B}}\mathbf{p}_0(0)$ is the vector sum of $-\mathcal{B}\mathbf{q}_1(0)$ and the mirror point of the vector $\mathcal{B}\mathbf{p}_1(0) = \mathcal{B}\mathbf{p}_0(0) + \mathcal{B}\mathbf{q}_1(0)$ with respect to plane orthogonal to $\boldsymbol{\omega}_e$. In particular, when $\mathcal{B}\mathbf{p}_1(0)$ lies in the plane orthogonal to $\boldsymbol{\omega}_e$, $\mathcal{B}\mathbf{p}_1(0)$ and its mirror point coincide, thereby removing the ambiguity. This is the case when the AUV moves in a horizontal plane. Thus, the range-only system in 2D is observable since the set of indistinguishable points contains only \mathbf{x}_0 . The above geometric interpretation can be exploited to show that a weakly observable system with a given trimming angular velocity (say $\boldsymbol{\omega}_e = \bar{\boldsymbol{\omega}}_e$), will become observable by instantaneously switching to another non-collinear trimming angular velocity $\boldsymbol{\omega}_e = \check{\boldsymbol{\omega}}_e$ such that $\bar{\boldsymbol{\omega}}_e \times \check{\boldsymbol{\omega}}_e \neq \mathbf{0}$. This means that the system can become observable by concatenating appropriately chosen, distinct trimming trajectories.

From Theorem 1 we obtain the following result for the particular case where the current is zero or known.

Corollary 1. *Consider the system (16) with range-only measurement, subject to constraints (11)-(13), and let all the requirements of Theorem 1 hold. Further assume that either there is no ocean current or $\mathcal{B}\boldsymbol{\nu}_c$ is known. Then for almost all inter-arrival times the system (16) is observable, provided*

$$\boldsymbol{\omega}'_e(\mathcal{B}\boldsymbol{\nu}_c + \boldsymbol{\nu}_e) \neq \mathbf{0}. \quad (20)$$

It is well known that the observability properties of a general nonlinear system depend on a particular actuator-sensor configuration. Furthermore, the introduction of additional sensors has the potential to improve the observability properties of the system. The next result shows that by including depth and range measurements, the system becomes observable. In what follows $\mathcal{I}_{rz}(\mathbf{x})$ denotes the set of indistinguishable states associated with the system (16) with range and depth measurements.

Theorem 2. *Consider the system (16) with range and depth measurements. Suppose that $\boldsymbol{\omega}_e \in \mathbb{R}^3$ satisfies (17) and the number of available samples of measurements on $[t_0, t_f]$ is at least 7 (that is $n_r \geq 7$). Moreover, let the inter-arrival times, $t_{k+1} - t_k$, be strictly positive. Then, for every $\mathbf{x}_0 \in \mathbb{R}^{12}$ and almost all inter-arrival times, $\mathcal{I}_{rz}(\mathbf{x}_0) = \{\mathbf{x}_0\}$ and the system is observable on $[t_0, t_f]$.*

The following corollary of Theorem 2 follows immediately.

Corollary 2. *Consider the system (16) and let all the requirements of Theorem 2 hold. Further, assume that either there is no ocean current or $\mathcal{B}\boldsymbol{\nu}_c$ is known. Then, for almost all inter-arrival times the system (16) is observable.*

Theorem 1 gives sufficient condition (17) for weak observability of system (16) subject to constraints (11)-(13) with range-only measurements. Further, introducing depth

measurements yields observability. This prompts the following question: If condition (17) is not satisfied, then what can be stated about the observability properties of system (16) with range (and depth) measurements? The next result discusses this case.

Theorem 3. *Consider the system (16) subject to constraints (11)-(13) and suppose that (17) does not hold. Then, the system subject to constraints (11)-(13) is not observable.*

Up until now we have investigated the case where the initial location of the beacon, $\mathcal{B}\mathbf{q}_1(0)$ is known and the initial position of the AUV, $\mathcal{B}\mathbf{p}_0(0)$ is unknown. We now consider the dual case, that is, $\mathcal{B}\mathbf{p}_0(0)$ is known but not the initial position of the beacon. The following result holds.

Theorem 4. *Consider the system (16), the constraints (11)-(13), and assume that $\mathcal{B}\mathbf{p}_0(0)$ is known. Then, (16) has observability properties similar to those obtained for the case where $\mathcal{B}\mathbf{q}_1(0)$ is known (see Theorems 1-3), except that the set of indistinguishable points is given by*

$$\mathcal{I}_r(\mathbf{x}_0) = \left\{ \mathbf{x}_0, \mathbf{x}_0 + \frac{2}{\boldsymbol{\omega}'_e\boldsymbol{\omega}_e} \begin{bmatrix} \mathbf{0} \\ -\boldsymbol{\omega}_e\boldsymbol{\omega}'_e(\mathcal{B}\mathbf{p}_0(0) + \mathcal{B}\mathbf{q}_1(0)) \\ -\boldsymbol{\omega}_e\boldsymbol{\omega}'_e(\mathcal{B}\boldsymbol{\nu}_c(0) + \boldsymbol{\nu}_e) \\ 2\boldsymbol{\nu}'_e\boldsymbol{\omega}_e\boldsymbol{\omega}'_e(\mathcal{B}\boldsymbol{\nu}_c(0) + \boldsymbol{\nu}_e) \\ \boldsymbol{\nu}'_e\boldsymbol{\omega}_e\boldsymbol{\omega}'_e(\mathcal{B}\mathbf{p}_0(0) + \mathcal{B}\mathbf{q}_1(0)) \\ \mathbf{0} \end{bmatrix} \right\}. \quad (21)$$

We are now ready to state the main result about system (14) which extends the previous results to more than one beacon.

Theorem 5. *Consider the system (14) with constant trimming linear velocity $\boldsymbol{\nu}_e \neq \mathbf{0}$, angular velocity $\boldsymbol{\omega}_e \in \mathbb{R}^3$ and constraints (11)-(13). Suppose that there is an anchor, that is, the initial condition $\mathcal{B}\mathbf{p}_0(0)$ or the position of one of the beacons $\mathcal{B}\mathbf{q}_i(0)$ is known. Assume that at least 7 samples of measurements, $n_r \geq 7$, are available on $[t_0, t_f]$ and let the inter-arrival times, $t_{k+1} - t_k$, be strictly positive. Suppose also that (17) holds. Then, for every $\mathbf{x}_0 \in \mathbb{R}^{12}$ and almost all inter-arrival times, the set of all initial conditions that are indistinguishable from $\mathbf{x}_0 \in [t_0, t_f]$ is given by $\mathcal{I}_{rz}(\mathbf{x}_0) = \{\mathbf{x}_0\}$.*

Under the same conditions, but with the assumption that only range measurements are available, it follows that the initial condition of each unknown vector in $\{\mathcal{B}\mathbf{p}_0, \mathcal{B}\mathbf{q}_i, \mathcal{B}\boldsymbol{\nu}_c; i = 1, 2, \dots, n\}$ has two possible solutions. Otherwise, if (17) does not hold, then the system subject to constraints (11)-(13) is not observable.

IV. OBSERVER DESIGN

This section addresses the problem of range-based localization system design by taking into consideration the results derived in the previous sections. Consider system (14), corrupted with deterministic but unknown bounded disturbance $\mathbf{d}: [0, t] \rightarrow \mathbb{R}^p$ and measurement noise $\mathbf{n}(t_k)$, that is,

$$\begin{cases} \dot{\mathbf{x}}(t) = A_{\mathbf{u}, \mathbf{y}}(t)\mathbf{x}(t) + \mathbf{b}_{\mathbf{u}}(t) + G_{\mathbf{u}}\mathbf{d}(t) \\ \mathbf{y}(t_k) = C_{\mathbf{u}}(t_k)\mathbf{x}(t_k) + \mathbf{n}(t_k) \end{cases} \quad (22)$$

The goal is to estimate the state vector $\mathbf{x}(t)$ given an initial estimate $\hat{\mathbf{x}}_0$ and the past control inputs and observations

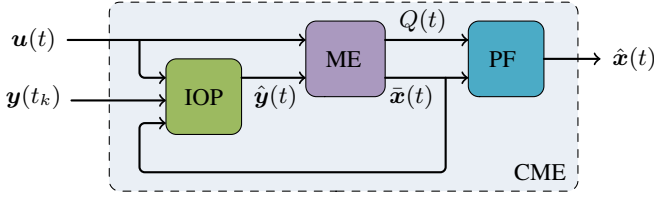


Fig. 2. Block diagram of the designed CME.

$\{\mathbf{u}(\tau), \mathbf{y}(t_\tau) : 0 \leq \tau \leq t, t_\tau \in \{t_1, \dots, t_k\} \subset [0, t]\}$, while satisfying the constraints (11)-(13).

To this effect, we propose the observer architecture depicted in Fig. 2, which will be henceforth referred to as the Constrained Minimum-Energy (CME) observer. The CME is composed of the following sub-systems:

- A Minimum-Energy Estimator (ME), whose role is to provide an estimate of the state $\bar{\mathbf{x}}(t)$ by solving in real time an unconstrained optimization problem (that will be defined later);
- A Projection Filter (PF), which maps an unconstrained solution $\bar{\mathbf{x}}(t)$ onto a constrained solution $\hat{\mathbf{x}}(t)$; and
- An Inter-sample Output Predictor (IOP), which provides a continuous estimate of the range measurement variable to be used by the ME estimator.

Later, we will *i*) extend the CME observer to deal with the problem of multiple beacons whose number is not known a-priori and can change over time and *ii*) use the concept of multiple-models to improve the convergence time of the proposed observer by taking into account the observability properties described in the previous sections.

A. Minimum-Energy Estimator (ME)

The ME estimator is formulated in a deterministic setting by producing an estimate for the state of the system that is *most compatible* with the system's dynamics and measured outputs. In particular, the optimal state estimate $\bar{\mathbf{x}}(t)$ is defined to be the value for the state that is compatible with the observations collected up to time t and the dynamics of the system, for the *lowest* possible measurement noise and disturbance, with *lowest* understood in an integral-square sense [18], [28]. More precisely, the state estimate $\bar{\mathbf{x}}$ is obtained from the solution of the optimization problem

$$\bar{\mathbf{x}}(t) = \arg \min_{\mathbf{z} \in \mathbb{R}^{n_s}} J(\mathbf{z}, t)$$

where the cost function $J(\mathbf{z}, t)$ is given by

$$J(\mathbf{z}, t) = \min_{\mathbf{d}, \mathbf{n}} \left\{ \|\mathbf{x}(0) - \bar{\mathbf{x}}_0\|_{Q_0} + \int_0^t \|\mathbf{d}(\tau)\|_{R_d}^2 d\tau + \sum_{k=1}^{k^*} \|\mathbf{n}(t_k)\|_{R_n}^2 : \mathbf{x}(t) = \mathbf{z}, \dot{\mathbf{x}} = A_{\mathbf{u}, \mathbf{y}} \mathbf{x} + \mathbf{b}_{\mathbf{u}}(t) + G_{\mathbf{u}} \mathbf{d}, \mathbf{y}(t_k) = C_{\mathbf{u}} \mathbf{x}(t_k) + \mathbf{n}(t_k) \right\} \quad (23)$$

with $Q_0 \succ 0$ and the index k^* satisfying $t_{k^*} = \lfloor t \rfloor$, where $\lfloor t \rfloor$ denotes the maximum discrete time $t_k \in [0, t)$, which is strictly less than t . The matrices $R_d, R_n \succ 0$ can be viewed as weighting parameters associated with the disturbances and

measurement noises. Using the results of [18], [28], [21], it can be concluded that this unconstrained state estimation problem has the following exact iterative solution:

- for $t_{k-1} \leq t < t_k$, $k = 1, \dots, k^*$

$$\begin{aligned} \dot{Q}(t) &= -A'_{\mathbf{u}, \mathbf{y}} Q(t) - Q(t) A_{\mathbf{u}, \mathbf{y}} - Q(t) G_{\mathbf{u}} R_d G'_{\mathbf{u}} Q(t) \\ \dot{\bar{\mathbf{x}}}(t) &= A_{\mathbf{u}, \mathbf{y}} \bar{\mathbf{x}}(t) + \mathbf{b}_{\mathbf{u}} \end{aligned} \quad (24)$$

- for $t = t_k$, $k = 1, \dots, k^*$

$$\begin{aligned} Q(t_k) &= Q(t_k^-) + C'_{\mathbf{u}} R_n^{-1} C_{\mathbf{u}} \\ \bar{\mathbf{x}}(t_k) &= \bar{\mathbf{x}}(t_k^-) + Q^{-1}(t_k) C'_{\mathbf{u}} R_n^{-1} (\mathbf{y}(t_k) - C_{\mathbf{u}} \bar{\mathbf{x}}(t_k^-)) \end{aligned} \quad (26)$$

while satisfying $Q(0) := Q_0 \succ 0$ and $\bar{\mathbf{x}}(0) := \bar{\mathbf{x}}_0$.

B. Projection Filter (PF)

In general, the solution obtained in the unconstrained state estimation problem $\bar{\mathbf{x}}(t)$ does not satisfy the constraints (11)-(13). To solve this problem, we first notice that (11)-(13) can be rewritten as quadratic constraints of the form $\mathbf{z}' S_i \mathbf{z} + \mathbf{r}'_i \mathbf{z} = 0$, $i \in \{1, \dots, 2n+1\}$. Thus, one strategy is to compute $\hat{\mathbf{x}}$ such that

$$\hat{\mathbf{x}}(t) = \arg \min_{\mathbf{z} \in \mathbb{R}^{n_s}; \forall l \in \{1, \dots, 2n+1\}} (\mathbf{z} - \bar{\mathbf{x}})' Q (\mathbf{z} - \bar{\mathbf{x}}). \quad (28)$$

Since (28) does not have a closed-form expression, following the ideas in [21], [29] we propose a scheme that solves asymptotically the related sufficient Karush-Kuhn-Tucker (KKT) conditions [30, pp 243–244]. More precisely, consider the Lagrangian function corresponding to the cost function in (28), that is,

$$\mathcal{L}(\hat{\mathbf{x}}, \boldsymbol{\lambda}) = (\hat{\mathbf{x}} - \bar{\mathbf{x}})' Q (\hat{\mathbf{x}} - \bar{\mathbf{x}}) + \sum_{i=1}^{2n+1} \lambda_i (\hat{\mathbf{x}}' S_i \hat{\mathbf{x}} + \mathbf{r}'_i \hat{\mathbf{x}})$$

where $\boldsymbol{\lambda} \in \mathbb{R}^{2n+1}$ is the Lagrange multiplier vector. This leads to the following sufficient KKT conditions for optimality:

$$\mathbf{e}_2 = \bar{Q} \hat{\mathbf{x}} - Q \bar{\mathbf{x}} + \bar{R} \boldsymbol{\lambda} = \mathbf{0}, \quad \mathbf{e}_3 = (\bar{S}(\hat{\mathbf{x}}) + 2\bar{R})' \hat{\mathbf{x}} = \mathbf{0}, \quad (29)$$

where

$$\begin{aligned} \bar{S}(\hat{\mathbf{x}}) &= [S_1 \hat{\mathbf{x}}, S_2 \hat{\mathbf{x}}, \dots, S_{2n+1} \hat{\mathbf{x}}], \\ \bar{R} &= [\mathbf{r}_1, \mathbf{r}_2, \dots, \mathbf{r}_{2n+1}] / 2, \quad \bar{Q} = Q + \sum_{i=1}^{2n+1} \lambda_i S_i. \end{aligned} \quad (30)$$

Suppose that along the trajectories of the system we have $\bar{Q} \succ 0$ and $\bar{S}(\hat{\mathbf{x}}) + \bar{R}$ remains full column rank. Then, setting the initial condition $\hat{\mathbf{x}}(0) = \bar{\mathbf{x}}_0$, the following proposed solution guaranties that the sufficient KKT conditions for (28) hold at sampling times $t = t_k$ and asymptotically in $[t_{k-1}, t_k)$, (i.e., \mathbf{e}_2 and \mathbf{e}_3 converge to zero as t_k goes to infinity):

- for $t_{k-1} \leq t < t_k$, $k = 1, \dots, k^*$

$$\begin{aligned} \begin{bmatrix} \dot{\hat{\mathbf{x}}} \\ \dot{\boldsymbol{\lambda}} \end{bmatrix} &= \begin{bmatrix} \bar{Q} & \bar{S}(\hat{\mathbf{x}}) + \bar{R} \\ \bar{S}(\hat{\mathbf{x}})' + \bar{R}' & \mathbf{0} \end{bmatrix}^{-1} \begin{bmatrix} -\bar{Q} \hat{\mathbf{x}} + Q \dot{\bar{\mathbf{x}}} + \bar{Q} \dot{\bar{\mathbf{x}}} \\ \mathbf{0} \end{bmatrix} \\ &\quad - \mu \begin{bmatrix} Q(\hat{\mathbf{x}} - \bar{\mathbf{x}}) + (\bar{S}(\hat{\mathbf{x}}) + \bar{R}) \boldsymbol{\lambda} \\ (\frac{1}{2} \bar{S}(\hat{\mathbf{x}}) + \bar{R})' \hat{\mathbf{x}} \end{bmatrix} \end{aligned} \quad (31)$$

- for $t = t_k$, $k = 1, \dots, k^*$

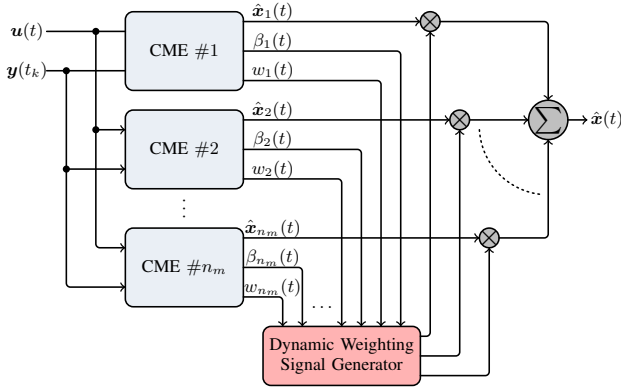


Fig. 3. Block diagram of the designed MMAE.

$$\begin{bmatrix} \hat{\mathbf{x}}(t_k) \\ \boldsymbol{\lambda}(t_k) \end{bmatrix} = \begin{bmatrix} \bar{Q}^{-1}(t_k) (Q(t_k)\bar{\mathbf{x}}(t_k) - \bar{R}\boldsymbol{\lambda}^*(t_k)) \\ \boldsymbol{\lambda}^*(t_k) \end{bmatrix} \quad (32)$$

where $\mu > 0$. The solution $\boldsymbol{\lambda}^*(t_k)$ is obtained by solving $f_l(\boldsymbol{\lambda}, t_k) = 0$, $l \in \{1, 2, \dots, 2n + 1\}$ using an iterative generalized Newton's method, where each f_l is given by

$$\begin{aligned} f_l(\boldsymbol{\lambda}, t_k) = & \bar{\mathbf{x}}' Q \bar{Q}^{-1} S_l \bar{Q}^{-1} Q \bar{\mathbf{x}} + \boldsymbol{\lambda}' \bar{R}' \bar{Q}^{-1} S_l \bar{Q}^{-1} \bar{R} \boldsymbol{\lambda} \\ & - 2(\bar{\mathbf{x}}' Q \bar{Q}^{-1} S_l + \mathbf{r}_l') \bar{Q}^{-1} \bar{R} \boldsymbol{\lambda} + 2\mathbf{r}_l' \bar{Q}^{-1} Q \bar{\mathbf{x}}. \end{aligned}$$

C. Inter-sample Output Predictor (IOP)

In (24)-(25) we assumed that the observation $\mathbf{y}(t)$ is piecewise continuous in time, which is not (it is a discrete signal). A straightforward approach to deal with this problem is to hold \mathbf{y} between sampling times. This, however, is not the best solution because it can introduce significant model mismatch if the inter-arrival times $t_{k+1} - t_k$ are not small enough. To overcome this problem, we suggest the use of an inter-sample output predictor such as the one described in [31]. For a general nonlinear system

$$\dot{\mathbf{x}}(t) = \mathbf{f}(\mathbf{x}(t), \mathbf{u}(t)), \quad \mathbf{y}(t_k) = \mathbf{h}(\mathbf{x}(t_k), \mathbf{u}(t_k))$$

the key idea consists of using the predicted output given by

$$\hat{\mathbf{y}}(t) = \nabla_{\hat{\mathbf{x}}} \mathbf{h}(\hat{\mathbf{x}}, \mathbf{u}(t)) \mathbf{f}(\hat{\mathbf{x}}(t), \mathbf{u}(t)), \quad \hat{\mathbf{y}}(t_k) = \mathbf{y}(t_k),$$

for $t \in [t_{k-1}, t_k)$. In our case, this corresponds to replacing the signals r_i in $A_{\mathbf{u}, \mathbf{y}}$ (see (10)) by \hat{r}_i , where

$$\begin{aligned} \dot{\hat{r}}_i(t) &= -(\boldsymbol{\nu}' (\mathcal{B} \mathbf{p}_i + \mathcal{B} \mathbf{q}_0) + \chi_c + \chi_{c_i}) / \hat{r}_i, \quad t \in [t_{k-1}, t_k), \\ \hat{r}_i(t_k) &= r_i(t_k). \end{aligned}$$

D. multiple-models

As discussed earlier, the process model (10) together with constraints (11)-(13) may not be observable, but only weakly observable (Theorem 1). In this case, the proposed CME converges to one of the two elements of $\mathcal{I}_r(\mathbf{x}_0)$ (see equations (18) and (21)), depending on the initial condition $\bar{\mathbf{x}}(0)$ of the observer. However, as soon as the system becomes observable, the state estimate will, as shown in the next section, converge to the true solution. In spite of this, there is still a problem of performance because the time that the estimate $\hat{\mathbf{x}}$ takes to reach a small neighborhood of the true solution \mathbf{x} depends on the magnitude of the initial state error $\|\hat{\mathbf{x}}(0) - \mathbf{x}(0)\|$.

This motivates the use of a Multiple-Model Adaptive Estimator (MMAE) [32] with the structure shown in Fig. 3. The MMAE consists of *i*) a bank of n_m local CME observers, where each observer is initialized with a different initial condition selected according to a suitable criterion (explained later) and *ii*) a dynamic weighting signal generator system that is responsible for updating the piecewise constant weights $p_s(t) \in [0, 1]$, $s = 1, 2, \dots, n_m$. The (final) state estimate $\hat{\mathbf{x}}(t)$ is given by a weighted sum of the local state estimates, that is,

$$\hat{\mathbf{x}}(t) = \sum_{s=1}^{n_m} p_s(t_k) \hat{\mathbf{x}}_s(t), \quad t \in [t_k, t_{k+1}),$$

where each $\hat{\mathbf{x}}_s(t)$, $s = 1, 2, \dots, n_m$ corresponds to a local state estimate generated by the s^{th} local CME observer. Following the approach in [32] but adapted to the problem of continuous dynamics with discrete measurements, the weights are piecewise constant signals that are updated at measurements times $t = t_k$ according to

$$p_s(t_k) = \frac{p_s(t_{k-1}) \beta_s(t_k) e^{-w_s(t_k)}}{\sum_{l=1}^{n_m} p_l(t_{k-1}) \beta_l(t_k) e^{-w_l(t_k)}}, \quad s \in \{1, 2, \dots, n_m\}$$

where $\beta_s(\cdot)$ is a positive bounded signal and $w_s(\cdot)$ is an error measuring function that maps the observations of the system and the states of the s^{th} local observer to a non-negative real value. Examples of $\beta_s(\cdot)$ and $w_s(\cdot)$ are

$$\begin{aligned} \beta_s(t_k) &= |\mathcal{S}_s(t_k)|^{-\frac{1}{2}}, \quad w_s(t_k) = \frac{1}{2} \|\hat{\mathbf{y}}_s(t_k^-) - \mathbf{y}(t_k)\|_{\mathcal{S}_s(t_k)}^2, \\ \mathcal{S}_s(t_k) &= C_{\mathbf{u}}(t_k) Q^{-1}(t_k) C_{\mathbf{u}}'(t_k) + R_{\mathbf{n}} > 0. \end{aligned}$$

In practice, to reduce memory and computing power, we have slightly modified the MMAE scheme according to the following procedure: Given the first range measurement obtained from a newly observed beacon i at time t_k , we generate two initial conditions for ${}^{\mathcal{B}}\bar{\mathbf{p}}_i(t_k)$ that satisfy constraints (11)-(13), using the expression (21) and an arbitrarily chosen ${}^{\mathcal{B}}\bar{\mathbf{p}}_i(t_k)$ (which is typically set to $[0, r_i(t_k), 0] + {}^{\mathcal{B}}\bar{\mathbf{q}}_0(t_k)$). Two new CME observers are then created with the corresponding initial condition. Then, we apply a MMAE scheme with the weights initialized with $p_1(t_k) = p_2(t_k) = 0.5$ (for the case of two models). Whenever one of the weights $p_s(\cdot)$ reaches some threshold near 1, the corresponding CME will be kept and all the other CMEs are discarded.

V. OBSERVER CONVERGENCE

In this section we investigate under what conditions the estimation error of the proposed observer converges to a small neighbourhood of zero (or zero, in the absence of the measurement noise and process disturbances). We first analyze the stability properties of each local CME observer.

A. Convergence of the CME observer

In what follows we assume the following:

Assumption 1. The matrix $\bar{Q}(t)$ defined in (30) is positive definite along the trajectories of the CME and $\bar{S}(\hat{\mathbf{x}}) + \bar{R}$ remains full column rank.

Assumption 2. Let $\text{Num}(t, \sigma)$, $0 \leq \sigma < t$ denote the number of time instants at which measurement arrive in the open interval

(σ, t) . There exist finite positive constants τ_D and N_0 , for which the following condition holds:

$$\text{Num}(t, \sigma) \leq N_0 + (t - \sigma) / \tau_D. \quad (33)$$

Regarding the first assumption, notice that Q is always positive definite, which means that $\bar{Q} > 0$ for λ sufficiently small. Also, the rank condition on $\bar{S}(\hat{x}) + \bar{R}$ is the standard condition on Lagrange multiplier theory for constraints independence, which in this case holds because each constraint is imposed on a different beacon. Assumption 2 typically arises in the context of logic-based switching control and also in estimation of continuous systems with discrete observations [18]. The constant τ_D is called the average dwell-time and N_0 the chatter bound. The condition above guarantees that the summation of $\|\mathbf{n}(\cdot)\|^2$ in (23) will not grow unbounded due to too frequent measurements. This assumption is purely technical and in practice always holds.

The next result establishes the convergence properties of the proposed CME observer. We will need the standard definition of class \mathcal{K} and \mathcal{KL} functions, see for instance [33, page 144].

Theorem 6. *Suppose that Assumptions 1-2 hold and denote $\mathbf{e}_1 := \bar{x} - x$. Let $\mathbf{u}(t)$, $\mathbf{y}(t_k)$ be a given input/output pair for system (22). Then, there exist a \mathcal{KL} function β and class \mathcal{K} functions γ_d , γ_n such that the estimation error associated with the CME observer satisfies*

$$\begin{aligned} \|\bar{\mathbf{e}}(t)\| \leq & \beta(\|\mathbf{e}(0)\|, t) + \gamma_d \left(\sup_{\tau \in [0, t]} \|\mathbf{d}(\tau)\|_{R_d^{-1}} \right) \\ & + \gamma_n \left(\sup_{t_\tau \in [0, t]} \|\mathbf{n}(t_\tau)\|_{R_n^{-1}} \right) \end{aligned} \quad (34)$$

where $\bar{\mathbf{e}} := [e'_1, e'_2, e'_3]'$ and $\mathbf{e}_2, \mathbf{e}_3$ are defined in (29).

Proof. Consider the following Lyapunov functions

$$V_1 = \mathbf{e}'_1 Q(t) \mathbf{e}_1, \quad V_2 = \mathbf{e}'_2 \mathbf{e}_2 / 2 + \mathbf{e}'_3 \mathbf{e}_3 / 2 \quad (35)$$

which are bounded below and above by some class \mathcal{K} functions. Consider first the case where $t \in [t_{k-1}, t_k]$ for some sampling times t_{k-1} and t_k . Computing the time derivative of V_1 and V_2 yields

$$\begin{aligned} \dot{V}_1 = & -\mathbf{e}'_1 (QA_{\mathbf{u}, \mathbf{y}} + A'_{\mathbf{u}, \mathbf{y}} Q + QG_{\mathbf{u}} R_d G'_{\mathbf{u}} Q) \mathbf{e}_1 \\ & + \mathbf{e}'_1 Q(A_{\mathbf{u}, \mathbf{y}} \mathbf{e}_1 - G_{\mathbf{u}} \mathbf{d}) + (A_{\mathbf{u}, \mathbf{y}} \mathbf{e}_1 - G_{\mathbf{u}} \mathbf{d})' Q \mathbf{e}_1 \\ = & -\frac{1}{2} \|G'_{\mathbf{u}} Q \mathbf{e}_1\|_{R_d}^2 - \frac{1}{2} \|G'_{\mathbf{u}} Q \mathbf{e}_1 + 2R_d^{-1} \mathbf{d}\|_{R_d}^2 + 2\|\mathbf{d}\|_{R_d^{-1}}^2, \\ \dot{V}_2 = & \mathbf{e}'_3 \left(2(\bar{S}(\hat{x}) + \bar{R})' \dot{\hat{x}} \right) \\ & + \mathbf{e}'_2 \left(\bar{Q} \dot{\hat{x}} - Q \dot{\hat{x}} + \dot{Q} \hat{x} - \dot{Q} \bar{x} + (\bar{S}(\hat{x}) + \bar{R}) \dot{\lambda} \right) \\ = & \begin{bmatrix} \mathbf{e}_2 \\ \mathbf{e}_3 \end{bmatrix} \left(\begin{bmatrix} \bar{Q} & \bar{S}(\hat{x}) + \bar{R} \\ \bar{S}(\hat{x})' + \bar{R}' & \mathbf{0} \end{bmatrix} \begin{bmatrix} \dot{\hat{x}} \\ \dot{\lambda} \end{bmatrix} + \begin{bmatrix} \dot{Q} \hat{x} - Q \dot{\hat{x}} - \dot{Q} \bar{x} \\ \mathbf{0} \end{bmatrix} \right). \end{aligned}$$

Using Assumption 1, equation (31), and the fact that $\delta I \leq G_{\mathbf{u}} R_d G'_{\mathbf{u}} \leq \Delta I$, we can conclude that

$$\dot{V}_1 \leq -\frac{1}{2} \delta \lambda_{\min}(Q) V_1 + 2\|\mathbf{d}\|_{R_d^{-1}}^2, \quad \dot{V}_2 = -2\mu V_2$$

where $\lambda_{\min}(Q)$ is the smallest eigenvalue of matrix Q . Notice that observability of the system (22) is a necessary and sufficient condition for $\lambda_{\min}(Q) > 0$. Defining

$\gamma := \frac{1}{2} \delta \inf_{\tau \in [t_{k-1}, t]} \lambda_{\min}(Q(\tau))$ we further conclude that

$$V_1(t) \leq V_1(t_{k-1}) e^{-\gamma(t-t_{k-1})} + \frac{2}{\gamma} \sup_{\tau \in [t_{k-1}, t]} \|\mathbf{d}(\tau)\|_{R_d^{-1}}^2, \quad (36)$$

$$V_2(t) = V_2(t_{k-1}) e^{-2\mu(t-t_{k-1})}, \quad (37)$$

for $t \in [t_{k-1}, t_k]$. Note that from (37) it follows that conditions (29) will be enforced (for sufficiently large μ and/or t_k).

Now consider the case where $t = t_k$. Using (27) we obtain

$$\mathbf{e}_1(t_k) = (I - Q^{-1}(t_k) \Psi(t_k)) \mathbf{e}_1(t_k^-) + Q^{-1}(t_k) \bar{\mathbf{n}}(t_k) \quad (38)$$

where $\bar{\mathbf{n}}(t_k) = C'_{\mathbf{u}} R_n^{-1} \mathbf{n}(t_k)$ and $\Psi(t_k) = C'_{\mathbf{u}} R_n^{-1} C_{\mathbf{u}}$. Thus, substituting (38) in (35) and considering the composite function $V = V_1 + V_2$ we obtain

$$\begin{aligned} V(t_k) = & \mathbf{e}_1(t_k^-)' (Q(t_k) + \Psi(t_k) Q^{-1}(t_k) \Psi(t_k) - 2\Psi(t_k)) \mathbf{e}_1(t_k^-) \\ & + 2\mathbf{e}_1(t_k^-)' (I - \Psi(t_k) Q^{-1}(t_k)) \bar{\mathbf{n}}(t_k) \\ & + \bar{\mathbf{n}}(t_k)' Q^{-1}(t_k) \bar{\mathbf{n}}(t_k) \\ & + \frac{1}{2} \|\bar{Q}(t_k) \hat{\mathbf{x}}(t_k) - Q(t_k) \bar{\mathbf{x}}(t_k)\|^2 + \frac{1}{2} \|\bar{S}(\hat{x})' \hat{x}\|^2 \end{aligned}$$

Notice that by using Assumption 1 and (32) it follows that $V_2(t_k) = 0$. Using the matrix inversion lemma [34] and (26) we can further simplify the terms in the above expression containing $Q(t_k)$ as

$$\begin{aligned} I - \Psi Q^{-1}(t_k) &= I - L' F L Q^{-1}, \\ Q(t_k) + \Psi Q^{-1}(t_k) \Psi - 2\Psi &= Q - L' F L, \\ Q^{-1}(t_k) &= Q^{-1} - Q^{-1} L' F L Q^{-1}, \end{aligned}$$

where $Q = Q(t_k^-)$, $L = \Psi^{\frac{1}{2}}(t_k)$ is any matrix such that $L'L = \Psi(t_k)$ and $F = (I + LQ^{-1}L')^{-1}$ is a positive definite matrix. This leads to

$$\begin{aligned} V(t_k) = & V_1(t_k^-) - \mathbf{e}_1(t_k^-)' (L' F L) \mathbf{e}_1(t_k^-) \\ & + 2\mathbf{e}_1(t_k^-)' (I - L' F L Q^{-1}) \bar{\mathbf{n}}(t_k) \\ & + \bar{\mathbf{n}}(t_k)' (Q^{-1} - Q^{-1} L' F L Q^{-1}) \bar{\mathbf{n}}(t_k) \\ \leq & V(t_k^-) + \bar{\mathbf{n}}(t_k)' Q^{-1} \bar{\mathbf{n}}(t_k) + 2\mathbf{e}_1(t_k^-)' \bar{\mathbf{n}}(t_k) \\ & - \|F^{\frac{1}{2}} L \mathbf{e}_1(t_k^-) - F^{\frac{1}{2}} L Q^{-1} \bar{\mathbf{n}}(t_k)\|^2 \\ \leq & (1 + \epsilon) V(t_k^-) + (1 + 1/\epsilon) \bar{\mathbf{n}}(t_k)' Q^{-1} \bar{\mathbf{n}}(t_k) \end{aligned} \quad (39)$$

where ϵ is an arbitrary small positive constant. Now, by combining (39) with (36)-(37) it follows that

$$\begin{aligned} V(t_k) \leq & (1 + \epsilon) [V_1(t_{k-1}) e^{-\gamma \Delta t_k} + V_2(t_{k-1}) e^{-2\mu \Delta t_k}] \\ & + (\epsilon + 1) a_k / \epsilon + b_k \end{aligned} \quad (40)$$

where $\Delta t_k = t_k - t_{k-1}$, $a_k = \lambda_{\max}(Q^{-1}) \|\bar{\mathbf{n}}(t_k)\|^2$, and $b_k = \frac{2(1+\epsilon)}{\gamma} \sup_{\tau \in [t_{k-1}, t_k]} \|\mathbf{d}(\tau)\|_{R_d^{-1}}^2$. Solving (40) recursively yields

$$\begin{aligned} V(t_k) \leq & (1 + \epsilon)^k [V_1(t_0) e^{\gamma(t_0 - t_k)} + V_2(t_0) e^{2\mu(t_0 - t_k)}] \\ & + \sum_{j=0}^{k-1} (1 + \epsilon)^j e^{\gamma(t_k - j - t_k)} ((\epsilon + 1) a_{k-j} / \epsilon + b_{k-j}) \end{aligned}$$

Using Assumption 2 (equation (33)) we can further simplify the above inequality to

$$\begin{aligned} V(t_k) \leq & \left[(1 + \epsilon)e^{-\gamma\tau_D} \right]^k e^{\gamma N_0 \tau_D} V_1(t_0) \\ & + \left[(1 + \epsilon)e^{-2\mu\tau_D} \right]^k e^{2\mu N_0 \tau_D} V_2(t_0) \\ & + \sum_{j=0}^{k-1} \left[(1 + \epsilon)e^{-\gamma\tau_D} \right]^j ((\epsilon + 1) a_{k-j} / \epsilon + b_{k-j}) e^{\gamma N_0 \tau_D} \end{aligned}$$

By choosing μ, ϵ such that $\kappa_1 := (1 + \epsilon)e^{-\gamma\tau_D} < 1$ and $\kappa_2 := (1 + \epsilon)e^{-2\mu\tau_D} < 1$ it follows that V is a bounded function and $V(t) \rightarrow \frac{1}{1 - \kappa_1} \left(\frac{\epsilon + 1}{\epsilon} \max_k a_k + \max_k b_k \right) e^{\gamma \max_k \{N_0 \tau_D\}}$ as $t \rightarrow \infty$. Using the fact that $\|\bar{e}\| \leq \|e_1\| + \|e_2\| + \|e_3\|$, we can now conclude inequality (34). \square

In Theorem 6 we have used the fact that Q is a positive definite matrix that is bounded below, which means that $\lambda_{\min}(Q) > 0$. This is true if the system is observable, that is, the observability matrix is full rank. This can be done either by using range and depth measurements or, in the case of range only measurements, by using at least two non-collinear piecewise constant angular velocities. Notice also that the estimate $\hat{x}(t)$ is the solution of the optimization problem (28) pointwise at times t_k and converges asymptotically to the optimal in the intervals $[t_{k-1}, t_k]$.

Remark 1. Consider system (10) without disturbance $\mathbf{d}(\cdot)$ and noise $\mathbf{n}(\cdot)$. In this case it can be concluded that as $t \rightarrow \infty$ the functions $V_1(t), V_2(t) \rightarrow 0$ which implies that $\bar{\mathbf{x}}(t) \rightarrow \mathbf{x}(t)$, $(\bar{S}(\hat{\mathbf{x}}(t)) + 2R)' \hat{\mathbf{x}}(t) \rightarrow 0$, from which it follows that $(\hat{\mathbf{x}} - \bar{\mathbf{x}})' Q (\hat{\mathbf{x}} - \bar{\mathbf{x}}) \rightarrow 0$. Since $Q \succ 0$, it follows that $\hat{\mathbf{x}}(t) \rightarrow \bar{\mathbf{x}}(t)$ and therefore $\hat{\mathbf{x}}(t) \rightarrow \mathbf{x}(t)$ as $t \rightarrow \infty$.

B. Convergence of the MMAE

So far we have investigated the convergence properties of each local CME observer, which implies that Theorem 6 and Remark 1 apply to each CME in the Multiple-Model approach. We now show that similar properties apply to the state estimate computed using the MMAE architecture. The next result provides conditions for the convergence of the dynamic weights $p_s(t)$. Roughly speaking, it says that the ‘‘model’’ identified is the one that exhibits least output error (residual) energy. The proof is omitted because it would be a slightly variation of the one in [32].

Lemma 1. Let $s^* \in \{1, \dots, n_m\}$ be an index corresponding to one of the CME observers, and let $\mathcal{S} = \{1, \dots, n_m\} \setminus \{s^*\}$ be an index set. Suppose that there exist positive constants n' and k' such that for all $k \geq k'$ and $n \geq n'$ the following condition holds for all $j \in \mathcal{S}$

$$\sum_{\tau=k}^{k+n-1} (w_{s^*}(t_\tau) - \ln \beta_{s^*}(t_\tau)) < \sum_{\tau=k}^{k+n-1} (w_j(t_\tau) - \ln \beta_j(t_\tau)) \quad (41)$$

Then $p_{s^*}(t) \rightarrow 1$ as $t \rightarrow \infty$.

Condition (41) can be viewed as a distinguishability criterion. The following result establishes the convergence of the proposed observer.

Theorem 7. Suppose that Assumptions 1-2 hold, and let $\mathbf{u}(t), \mathbf{y}(t_k)$ be a given input/output pair of system (22). Then, there exist a \mathcal{KL} function β , and class \mathcal{K} functions γ_d, γ_n such that the estimation error associated with the MMAE is bounded and satisfies

$$\begin{aligned} \|\mathbf{e}_M(t)\| \leq & \beta(\|\mathbf{e}_M(0)\|, t) + \gamma_d \left(\sup_{\tau \in [0, t]} \|\mathbf{d}(\tau)\|_{R_d^{-1}} \right) \\ & + \gamma_n \left(\sup_{t_\tau \in [0, t]} \|\mathbf{n}(t_\tau)\|_{R_n^{-1}} \right) \end{aligned} \quad (42)$$

where $\mathbf{e}_M(t)$ is the weighted sum of the error vectors associated to each model defined in Theorem 6, that is,

$$\mathbf{e}_M(t) := \sum_{s=1}^{n_m} p_s(t) \bar{\mathbf{e}}_s(t) \quad (43)$$

Suppose also that the distinguishability criterion (41) holds. Then, there exists an index $s^* \in \{1, 2, \dots, n_m\}$ such that $\mathbf{e}_M(t) \rightarrow \bar{\mathbf{e}}_{s^*}(t)$ as $t \rightarrow \infty$.

Proof. From (43) and (34) we can conclude that

$$\begin{aligned} \|\mathbf{e}_M(t)\| \leq & \sum_{s=1}^{n_m} p_s(t) \left(\beta_s(\|\bar{\mathbf{e}}_s(0)\|, t) + \gamma_{d_s} \left(\sup_{\tau \in [0, t]} \|\mathbf{d}(\tau)\|_{R_d^{-1}} \right) \right. \\ & \left. + \gamma_{n_s} \left(\sup_{t_\tau \in [0, t]} \|\mathbf{n}(t_\tau)\|_{R_n^{-1}} \right) \right) \end{aligned}$$

for some $\beta_s \in \mathcal{KL}$ and $\gamma_{d_s}, \gamma_{n_s} \in \mathcal{K}$, $s \in \{1, 2, \dots, n_m\}$. Thus, there exist class \mathcal{KL} function β and class \mathcal{K} functions γ_d, γ_n such that (42) holds. Now, if the distinguishability criterion (41) holds, we can conclude that $p_{s^*} \rightarrow 1$ and $p_s \rightarrow 0, \forall s \in \mathcal{S}$. This implies that $\mathbf{e}_M(t) \rightarrow \bar{\mathbf{e}}_{s^*}(t)$ as $t \rightarrow \infty$. \square

VI. EXPERIMENTAL RESULTS

In this section we describe a set of experiments carried out with three autonomous marine vehicles of the MEDUSA class, developed at IST (see Fig. 4). Each vehicle has two side thrusters that can be independently controlled to impart forward and rotational motion and is equipped with an attitude and heading reference unit (AHRS) that provides measurement of body orientation $\boldsymbol{\eta}(t)$ and angular velocity $\boldsymbol{\omega}(t)$. To obtain the forward velocity $\nu(t)$, and since this class of vehicles do not carry a Doppler velocity logger, an on-line computational procedure was used to estimate it based on the readings of the commands that are sent to the thrusters and using a quasi steady-state model of the vehicle [35]. A GPS module was used for ground truth comparison purposes. Each vehicle is equipped with an acoustic Tritech Micron data modem and ranging unit that is used for communications and also to measure the ranges among vehicles. The tests were performed in open water, in June 2012 at the Expo area of Lisbon, Portugal (Lat: 38.766 Long: -9.03) (see Fig. 4 left). See [17], [35] for more information on MEDUSA autonomous marine vehicles and the experimental site in Lisbon. Throughout the tests, two of the MEDUSA vehicles were kept in a hold position mode to act as proxies for stationary beacons. The other MEDUSA maneuvers at the surface and acts as proxy for an underwater vehicle moving at constant depth, interrogating the

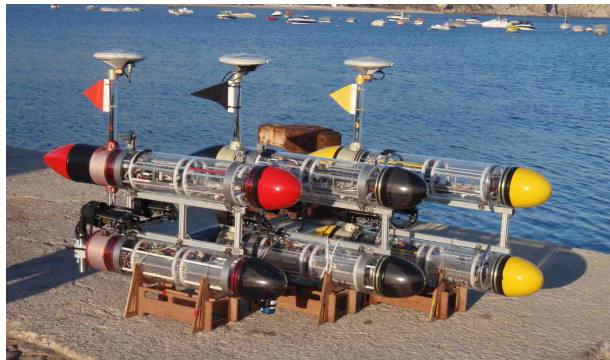


Fig. 4. The three MEDUSA marine robotic vehicles.

beacons. This is realistic, because the vehicle does not use GPS or aerial communications for localization purposes.

Due to space limitations, only three types of trajectories for the moving MEDUSA are described below:

- 1) A lawn-mower trajectory (see Fig. 5) where the observability conditions are not satisfied initially. However, as soon as the AUV turns, the observability condition (17) holds.
- 2) A small circular trajectory performed with (commanded) angular velocity $\omega_{e_z} = 0.025[\text{rad/s}]$ (see Fig. 7). The observability condition is satisfied from the time the AUV starts.
- 3) A larger circumference performed with (commanded) angular velocity $\omega_{e_z} = 0.012[\text{rad/s}]$ (see Fig. 8). Since the angular velocity ω_{e_z} is smaller, when compared to the second mission, different results are expected.

The moving MEDUSA, which starts at the initial position identified by the symbol (\square), moves with a commanded forward velocity of $0.5[\text{m/s}]$ and interrogates each beacon in cycles of 4 seconds, which guaranties that the inter-arrival time condition (45) holds. After extensive trials we concluded that the range measurements acquired by the modems can be modeled as being corrupted with additive noise with a bounded error of $0.3[\text{m}]$. In these experiments it was observed that the movement of the AUV was affected by constant ocean currents. Thus, without the knowledge of the ocean current vector, the dead reckoning error accumulates very fast (see the dead reckoning error in Fig. 5-8).

The local estimators in the proposed multiple-model observer approach are initialized as described in Section IV, meaning that one of the initial estimates of the position of each beacon is on the left hand side of the AUV and the other one on the right. The design parameters for the observers were set to $Q(0) = \text{diag}([10^2 I_2, 10^{-2} I_4, 10^2 I_2, 0.1 I_3, 10 I_2])$, $R_n = 0.25 I_2$, $R_d = \text{diag}([5 \times 10^{-3} I_2, 10^{-6} I_6, 0.1 I_3, 10^{-6}, 10^{-4} I_2])$, and $\mu = 10$ in the appropriate units.

1) *Mission 1*: Fig. 5 shows the trajectory of the AUV (GPS, estimated trajectory using dead reckoning only, and estimated trajectory using the proposed observer), the beacon locations (the true locations and their estimates), estimation errors, and estimated current velocity for mission 1. Clearly, as soon as the vehicle turns and therefore the system becomes observable,

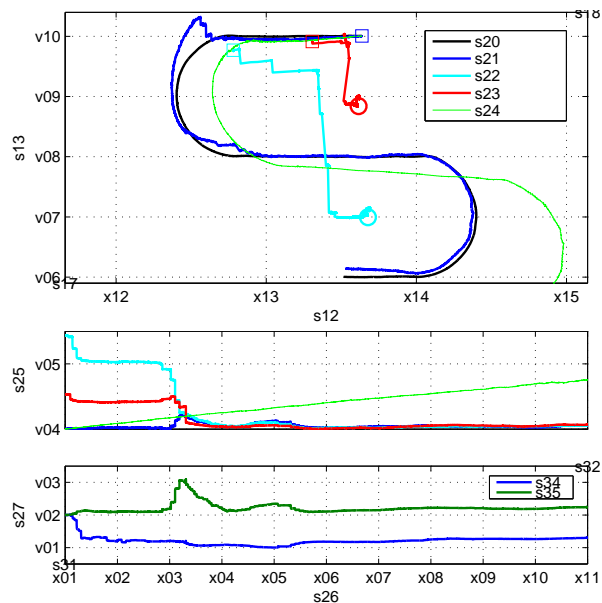


Fig. 5. Mission 1: Top) Trajectory of the AUV (GPS, estimated using dead reckoning only and estimated using the proposed observer) and beacon locations (true position denoted by 'O', and estimated with initial condition ' \square '); Bottom) Estimation errors, and estimated current velocity.

the estimation error of the observer initialized with arbitrary chosen initial condition converges to a small value close to zero. This can also be seen in the evolution of the estimated state of each local estimator, shown in Fig. 6. In this case, model 1 converges to the true locations of the beacons, while the other models converge to some or all of the mirror points for each beacon. The evolution of the models weights is shown in Fig. 10, where the weight of model 1 converges to 1 since it has the least error function.

2) *Mission 2*: In this mission, see Fig. 7, $\omega_{e_z} > 0$ and therefore the observability condition (17) holds. Thus, convergence of the estimator is achieved much faster when compared to the first mission. This can also be observed from the convergence of the models' weights depicted in Fig. 10.

3) *Mission 3*: In the last mission, the AUV moves on a larger circumference, with an average angular velocity which is half of that in the second mission (see Fig. 8). Although convergence of the models' weights is similar to that observed in mission 2 (note Fig. 10), the same is not true for the

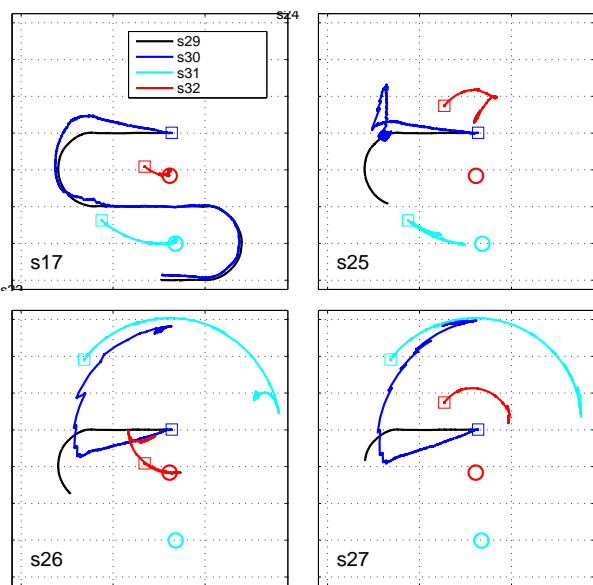


Fig. 6. Evolution of the AUV and estimated beacon positions for each model presented in the XY plane, corresponding to mission 1.

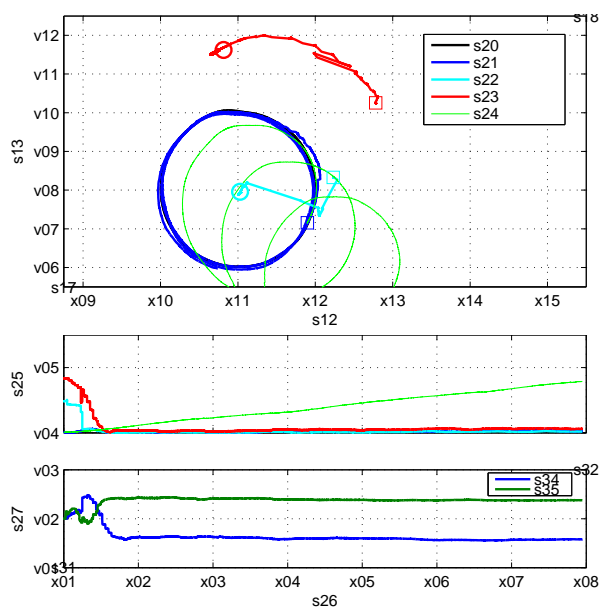


Fig. 7. Mission 2: Top) Trajectory of the AUV (GPS, estimated using dead reckoning only and estimated using the proposed observer) and beacon locations (true position denoted by 'O', and estimated with initial condition '□'); Bottom) Estimation errors, and estimated current velocity.

convergence of the states errors, which is slower. This is due to the smaller magnitude of the angular velocity ω_{e_z} which leads to an observability matrix with higher condition number and smaller minimum singular value. These two values are a measure of the quality of the unobservability of the system and the corresponding estimator. The reader is referred to [36], [37] for a discussion of these unobservability measures.

In Fig. 11 we compare the effect of disabling one or more of the designed blocks in the three missions. We consider five observers: i) Complete observer consisting of the ME, PF, IOP, and MMAE blocks; ii) Observer without the IOP module; iii) Observer without using the PF module, which solves the

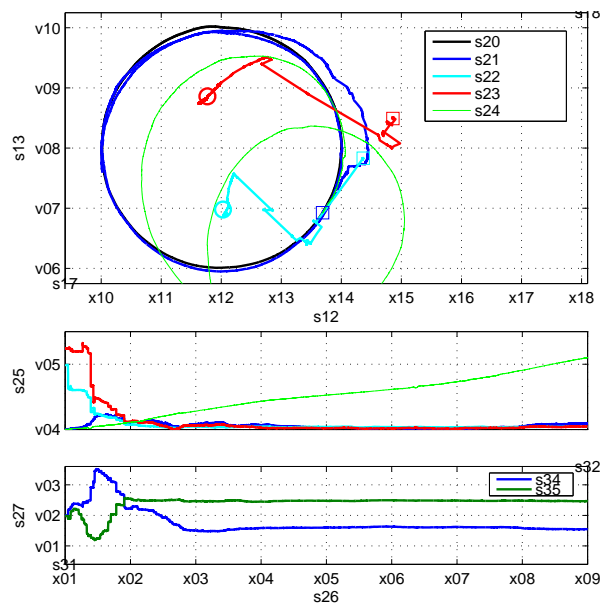


Fig. 8. Mission 3: Top) Trajectory of the AUV (GPS, estimated using dead reckoning only and estimated using the proposed observer) and beacon locations (true position denoted by 'O', and estimated with initial condition '□'); Bottom) Estimation errors, and estimated current velocity.

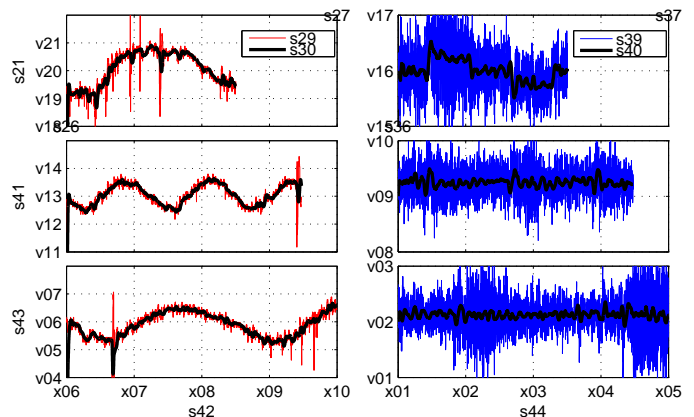


Fig. 9. Linear and angular velocities of the AUV for missions 1-3. Filtered data are shown with a black solid line.

unconstrained problem; iv) Observer with only the ME and the MMAE module; v) Plain ME observer. As expected, the fact of taking into account the quadratic constraint together with the IOP and the MMAE along with the ME observer improves significantly the convergence of the estimation error during the transient phase, when compared with the unconstrained ME observer. Notice also in missions 2 and 3 that after sufficient time has elapsed there is no significant difference in the performance of these observers. This shows that the output of the PF, \hat{x} , converges to the output of ME, \bar{x} , meaning that \hat{x} satisfies the constraints (11)-(13).

VII. CONCLUSIONS

The paper addressed theoretical and practical issues related to the problem of range-based simultaneous AUV/multi beacon localization in the presence of ocean currents. Conditions

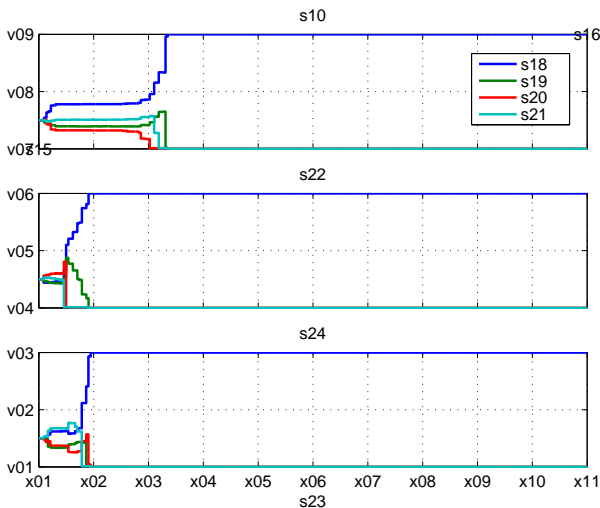


Fig. 10. Time evolution of the models weights for missions 1-3.

were derived under which it is possible to reconstruct the initial condition of the system under study. The latter includes the position of the beacons and the vehicle. In the model adopted for localization system design, the states evolve continuously with time but the range measurements are only available at discrete instants of time, in a possible non-uniform manner. Motivated by practical considerations that have to do with maneuverability and energy related issues, we considered the important case where the AUV undergoes motion along trimming trajectories. We have shown that this class of trajectories, which are sufficiently general to be of practical use, allow for a simple characterization of the types of maneuvers that yield observability or weak observability of the underlying design model. In particular, we proved that generically, for an arbitrary range measurement schedule, if either the position of one of the beacons or the initial position of the AUV are known, then there are trimming trajectories such that even without depth information the model is weakly observable. In the process of deriving these results, we obtained a complete mathematical characterization of the unobservable space and interpreted it geometrically. If depth measurements are also available, then the mode is observable even in the presence of unknown constant ocean currents. The results derived have a strong practical implication in that the concatenation of at least two appropriately chosen different trimming trajectories that do not necessarily yield observability individually, leads to an observable system. Equipped with these results, in the second part of the paper we proposed a novel multiple-model observer for simultaneous AUV and beacon localization. The set-up adopted was motivated by the fact that some of the trajectories used may yield temporary unobservability over a finite interval of time, thus warranting the use of multiple-models running in parallel. The resulting observer borrows concepts from minimum-energy estimation theory, projection filters, and multiple-model estimation techniques. Convergence analysis of the resulting observer system was formally done. The results of field experiments with a robotic marine vehicle showed the efficacy of the simultaneous AUV/multiple beacon

localization system.

ACKNOWLEDGMENT

The authors gratefully acknowledge the DSOR team for their efforts in the development of the MEDUSA vehicles and their support and collaboration on the planning and execution of our sea trials, F. Almeida, J. Botelho, P. Góis, M. Ribeiro, J. Ribeiro, M. Rufino, L. Sebastião, H. Silva, and J. Soares. This work was supported in part by projects EC CADDY (FP7-ICT-2013, Grant Agreement No. 611373) and the FCT [UID/EEA/50009/2013]. The first author benefited from a PhD scholarship of the Foundation for Science and Technology (FCT), Portugal.

APPENDIX

The following proposition is instrumental in analyzing the impact of the sampling times on the observability properties of the systems (14) and (16).

Proposition 1. *Consider $w > 0$, and let $t_1 < t_2 < \dots < t_n$, $n \geq 7$ be consecutive sampling times. Then the matrix $\mathcal{O}_t \in \mathbb{R}^{n \times 7}$, composed by rows of the form*

$$\mathcal{O}_{t_i} = [1 \quad t_i \quad t_i^2 \quad \sin(t_i w) \quad \cos(t_i w) \quad t_i \sin(t_i w) \quad t_i \cos(t_i w)],$$

is full column rank, except on a zero measure set given by $|\mathcal{O}_t| = 0$ with

$$\bar{\mathcal{O}}_t = \begin{bmatrix} A & B \\ C & D \end{bmatrix}, A = \begin{bmatrix} \bar{\beta}_{42} - \bar{\beta}_{32} & \bar{\alpha}_{42} - \bar{\alpha}_{32} \\ \bar{\beta}_{52} - \bar{\beta}_{42} & \bar{\alpha}_{52} - \bar{\alpha}_{42} \end{bmatrix}, B = \begin{bmatrix} \bar{\beta}_{41} - \bar{\beta}_{31} & \bar{\alpha}_{41} - \bar{\alpha}_{31} \\ \bar{\beta}_{51} - \bar{\beta}_{41} & \bar{\alpha}_{51} - \bar{\alpha}_{41} \end{bmatrix}, \\ C = \begin{bmatrix} \bar{\beta}_{62} - \bar{\beta}_{52} & \bar{\alpha}_{62} - \bar{\alpha}_{52} \\ \bar{\beta}_{72} - \bar{\beta}_{62} & \bar{\alpha}_{72} - \bar{\alpha}_{62} \end{bmatrix}, D = \begin{bmatrix} \bar{\beta}_{61} - \bar{\beta}_{51} & \bar{\alpha}_{61} - \bar{\alpha}_{51} \\ \bar{\beta}_{71} - \bar{\beta}_{61} & \bar{\alpha}_{71} - \bar{\alpha}_{61} \end{bmatrix},$$

and $\bar{\beta}_{ij} = \frac{\sin(t_i w) - \sin(t_j w)}{t_i - t_j}$, $\bar{\alpha}_{ij} = \frac{\cos(t_i w) - \cos(t_j w)}{t_i - t_j}$. In particular, suppose the inter-arrival times are uniform, that is, $t_{k+1} - t_k = T$ for all $t_k \in [t_0, t_f)$. Then, the matrix \mathcal{O}_t is full column rank except on a zero measure set described by (19).

Proof. Consider the following matrices P_1, P_2, P_3, P_4 , and P_5 defined as

$$P_1 := I_7 - \begin{bmatrix} 0 & t_1 I_2 & s_1 & c_1 & 0 \\ 0 & 0 & 0 & 0 & 0 \\ 0 & 0 & 0 & 0 & t_1 I_2 \\ 0 & 0 & 0 & 0 & 0 \end{bmatrix}, P_2 := I_6 - \begin{bmatrix} 0 & t_2 & \bar{\beta}_{21} & \bar{\alpha}_{21} & s_2 & c_2 \\ 0 & 0 & 0 & 0 & 0 & 0 \end{bmatrix}, \\ P_3 := I_5 - \begin{bmatrix} 0 & \bar{\gamma}_{32} & \bar{\nu}_{32} & \bar{\beta}_{32} & \bar{\alpha}_{32} \\ 0 & 0 & 0 & 0 & 0 \end{bmatrix}, P_4 := I_4 - \begin{bmatrix} 0 & 0 \\ I_3 & 0 \end{bmatrix}, P_5 := \begin{bmatrix} 0 & (t_1 - t_2) I_2 \\ I_2 & I_2 \end{bmatrix},$$

where $s_i = \sin(t_i w)$, $c_i = \cos(t_i w)$, $\bar{\gamma}_{j2} = \frac{\bar{\beta}_{j1} - \bar{\beta}_{21}}{t_j - t_2}$, $\bar{\nu}_{j2} = \frac{\bar{\alpha}_{j1} - \bar{\alpha}_{21}}{t_j - t_2}$, $i \in \{1, \dots, 7\}$, $j \in \{3, \dots, 7\}$.

Notice that the determinant of the above matrices with exception of P_5 is one, that is, $|P_5| = (t_2 - t_1)^2 > 0$. Thus, we may conclude that the determinant of \mathcal{O}_t , composed by

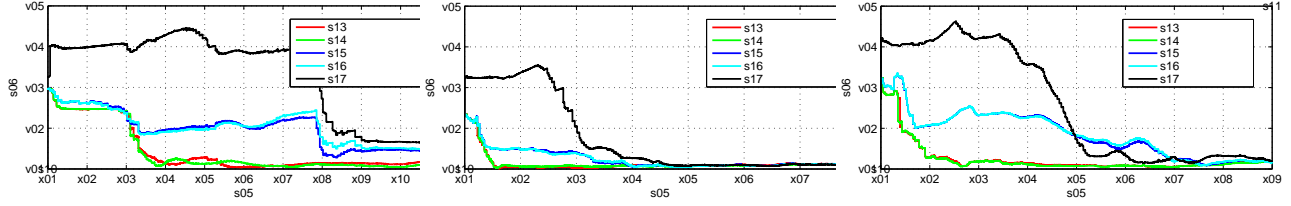


Fig. 11. Comparison of different methods for missions 1-3.

the first 7 row vectors $\mathcal{O}_{t_i}, i \in \{1, 2, \dots, 7\}$, satisfies

$$\begin{aligned}
 |\mathcal{O}_t| &= |\mathcal{O}_t \cdot P_1| = \prod_{i=2}^7 (t_i - t_1) \begin{vmatrix} 1 & t_2 & \bar{\beta}_{21} & \bar{\alpha}_{21} & s_2 & c_2 \\ \vdots & \vdots & \vdots & \vdots & \vdots & \vdots \\ 1 & t_7 & \bar{\beta}_{71} & \bar{\alpha}_{71} & s_7 & c_7 \end{vmatrix} \cdot P_2 \\
 &= \prod_{i=2}^7 (t_i - t_1) \prod_{i=3}^7 (t_i - t_2) \begin{vmatrix} 1 & \bar{\gamma}_{32} & \bar{\nu}_{32} & \bar{\beta}_{32} & \bar{\alpha}_{32} \\ \vdots & \vdots & \vdots & \vdots & \vdots \\ 1 & \bar{\gamma}_{72} & \bar{\nu}_{72} & \bar{\beta}_{72} & \bar{\alpha}_{72} \end{vmatrix} \cdot P_3 \\
 &= (t_2 - t_1)^{-2} \prod_{i=2}^7 (t_i - t_1) \prod_{i=3}^7 (t_i - t_2) \\
 &\quad \begin{vmatrix} P_4 \cdot \begin{bmatrix} \bar{\gamma}_{42} - \bar{\gamma}_{32} & \bar{\nu}_{42} - \bar{\nu}_{32} & \bar{\beta}_{42} - \bar{\beta}_{32} & \bar{\alpha}_{42} - \bar{\alpha}_{32} \\ \bar{\gamma}_{52} - \bar{\gamma}_{32} & \bar{\nu}_{52} - \bar{\nu}_{32} & \bar{\beta}_{52} - \bar{\beta}_{32} & \bar{\alpha}_{52} - \bar{\alpha}_{32} \\ \bar{\gamma}_{62} - \bar{\gamma}_{32} & \bar{\nu}_{62} - \bar{\nu}_{32} & \bar{\beta}_{62} - \bar{\beta}_{32} & \bar{\alpha}_{62} - \bar{\alpha}_{32} \\ \bar{\gamma}_{72} - \bar{\gamma}_{32} & \bar{\nu}_{72} - \bar{\nu}_{32} & \bar{\beta}_{72} - \bar{\beta}_{32} & \bar{\alpha}_{72} - \bar{\alpha}_{32} \end{bmatrix} \\ P_5 \end{vmatrix} \cdot P_5 \\
 &= (t_2 - t_1)^{-2} \prod_{i=2}^7 (t_i - t_1) \prod_{i=3}^7 (t_i - t_2) |\bar{\mathcal{O}}_t|. \quad (44)
 \end{aligned}$$

Since $t_i \neq t_j$ for all $i \neq j$, first term on the right hand side of (44) is nonzero.

Now consider the vector of inter-arrival times $\tilde{t} \in \mathbb{R}_+^6$ where $\tilde{t}_i = t_{i+1}w - t_iw$, $i \in \{1, 2, \dots, 6\}$. The determinants of the matrices A and $\bar{\mathcal{O}}_t$ can be written as $|A| = f_1 \sin(\tilde{t}_2) + f_2 \sin^2(\tilde{t}_2/2) + f_3 \tilde{t}_2$ and $|\bar{\mathcal{O}}_t| = \tilde{f}_4 \sin(\tilde{t}_6) + \tilde{f}_6 \sin^2(\tilde{t}_6/2) + \tilde{f}_8 \tilde{t}_6$, where $\tilde{f}_i := f_i + f_{i+1} \tilde{t}_6$, $i \in \{4, 6, 8\}$. Notice that f_1, f_2 , and f_3 are continuous functions of \tilde{t}_3 , and \tilde{t}_4 and f_4, \dots, f_9 are continuous functions of $\tilde{t}_1, \dots, \tilde{t}_5$. Furthermore, for any given \tilde{t}_3 and \tilde{t}_4 , $|A|$ has countable zero crossings. Since f_1, f_2 , and f_3 are continuous functions of \tilde{t}_3 and \tilde{t}_4 , we can conclude that the set of points satisfying $|A| = 0$ is composed of a number of countable surfaces in \mathbb{R}_+^3 , and is therefore a zero measure set. Using the same reasoning as for matrix A , it can be concluded that the set of points satisfying $|\bar{\mathcal{O}}_t| = 0$ also has zero measure. Thus, the matrix \mathcal{O}_t is generically of full column rank, losing rank only at the set of zero measure sample points given by $|\bar{\mathcal{O}}_t| = 0$.

Consider the particular case where the inter-arrival times are uniform, that is, $t_{k+1} - t_k = T$ for all $t_k \in [t_0, t_f]$. Then, it follows that $|\bar{\mathcal{O}}_t(T)| = 2^{15} T^{-4} \sin^{12}(T\|\omega_e\|/2) \sin^4(T\|\omega_e\|)$. This implies that the matrix \mathcal{O}_t is of full column rank almost everywhere, losing rank only at the zero measure sample points described by the set (19). \square

In Proposition 1 we showed that the matrix \mathcal{O}_t is full rank almost everywhere except at a set of particular sample times of zero measure defined by $|\bar{\mathcal{O}}_t| = 0$. Thus, even if the matrix $\bar{\mathcal{O}}_t$ is singular at a particular combination of sampling times, by slightly perturbing the sample times it becomes non-singular. For the non-uniform case, it is still possible to conclude numerically that for all the points in the region defined by

$$0 < t_{k+1} - t_k < \kappa\pi\|\omega_e\|^{-1}, \quad t_k \in [t_0, t_f] \quad (45)$$

for $\kappa = 0.9$ and at least 6 inter-arrival times, $|\bar{\mathcal{O}}_t| \neq 0$.

Proof. [**Theorem 1**] Consider system (16) with initial condition $x_0 \in \mathbb{R}^{12}$. Let $\omega_e \in \mathbb{R}^3$ be such that (17) holds. Without loss of generality we consider $t_0 = 0$. The state transition matrix $\Phi(t, 0) \in \mathbb{R}^{12 \times 12}$ of (16) is given by

$$\Phi(t, 0) = \begin{bmatrix} \bar{\Phi}_1(t, 0) & 0 & -t\bar{\Phi}_1(t, 0) & 0 & 0 & 0 \\ 0 & \bar{\Phi}_1(t, 0) & 0 & 0 & 0 & 0 \\ 0 & 0 & \bar{\Phi}_1(t, 0) & 0 & 0 & 0 \\ 0 & 0 & 0 & 1 & 0 & 0 \\ 0 & 0 & \frac{\bar{\Phi}_2(t, 0)}{2} & -t & 1 & 0 \\ \bar{\Phi}_2(t, 0) & \bar{\Phi}_2(t, 0) & -t\bar{\Phi}_2(t, 0) & t^2 & -2t & 1 \end{bmatrix} \quad (46)$$

where $\bar{\Phi}_1(t, 0)$ is the state transition matrix of the linear system $\dot{\zeta} = -S(\omega_e)\zeta$ and $\bar{\Phi}_2(t, 0) = -2 \int_0^t \nu'_e \bar{\Phi}_1(s, 0) ds$. The observability matrix $\mathcal{O}_{n_r} \in \mathbb{R}^{n_r \times 12}$, $n_r \geq 7$ associated with the system (16) is, according to [38], defined by

$$\mathcal{O}_{n_r} := [(C_u(t_0)\Phi(t_0, 0))' \quad \dots \quad (C_u(t_{n_r-1})\Phi(t_{n_r-1}, 0))']',$$

where $t_k \in [t_0, t_f]$, $k \in \{0, 1, 2, \dots, n_r - 1\}$. Note that \mathcal{O}_{n_r} is a function of the measurement sampling times, $t_k \in [t_0, t_f]$.

We claim that \mathcal{O}_{n_r} has rank 7 almost everywhere, with the exception of a zero measure set. We show this by using the rank-factorization theorem in [34, Theorem 3.13]. Note that $\mathcal{O}_{n_r} = \mathcal{O}_t(t_j, \|\omega_e\|)\mathcal{O}_r$, $j \in \{0, 1, \dots, n_r - 1\}$, where $\mathcal{O}_t \in \mathbb{R}^{n_r \times 7}$ whose j^{th} row, \mathcal{O}_{t_j} , is given by

$$\mathcal{O}_{t_j} := 2\nu_e \begin{bmatrix} \frac{1}{2\nu_e} & t_j & \frac{1 - \cos(t_j\|\omega_e\|)}{\|\omega_e\|^2} & \frac{t_j\|\omega_e\| - \sin(t_j\|\omega_e\|)}{\|\omega_e\|^3} \\ \frac{t_j^2}{2\|\omega_e\|^2} & t_j \frac{\cos(t_j\|\omega_e\|) - 1}{\|\omega_e\|^2} & \frac{t_j \sin(t_j\|\omega_e\|)}{\|\omega_e\|^3} \end{bmatrix}$$

and $\mathcal{O}_r \in \mathbb{R}^{7 \times 12}$ is given by

$$\mathcal{O}_r = \begin{bmatrix} 0 & 0 & 0 & 0 & 0 & 1 \\ -e'_x & -e'_x & 0 & 0 & \frac{-1}{\nu_e} & 0 \\ e'_x \times \omega'_e & e'_x \times \omega'_e & 0 & 0 & 0 & 0 \\ \omega'_e \omega_e e'_x - e'_x \omega_e \omega'_e & \omega'_e \omega_e e'_x - e'_x \omega_e \omega'_e & 0 & 0 & 0 & 0 \\ 0 & 0 & 2e'_x \omega_e \omega'_e & \frac{\|\omega_e\|^2}{\nu_e} & 0 & 0 \\ 0 & 0 & e'_x \times \omega'_e & 0 & 0 & 0 \\ 0 & 0 & \omega'_e \omega_e e'_x - e'_x \omega_e \omega'_e & 0 & 0 & 0 \end{bmatrix}.$$

Resorting to Proposition 1 it can be concluded that for almost all inter-arrival times $\text{Rank}(\mathcal{O}_t) = 7$. Moreover, from (17) it follows that $\text{Rank}(\mathcal{O}_r) = 7$. Thus, by the rank factorization theorem it follows that $\text{Rank}(\mathcal{O}_{n_r}) = \text{Rank}(\mathcal{O}_r)$.

Since $\text{Rank}(\mathcal{O}_{n_r}) = \text{Rank}(\mathcal{O}_r)$, we can conclude that $\text{Kernel}(\mathcal{O}_{n_r}) = \text{Kernel}(\mathcal{O}_r)$. Thus, the null space associated with the observability matrix is $\text{Kernel}(\mathcal{O}_{n_r}) = \mathcal{N}\alpha$ where

$$\mathcal{N} = \begin{bmatrix} e_x & (e_x \times \omega_e)\omega_{e_z} & -(e_x \times \omega_e)\omega_{e_y} & \omega_e - e_x e'_x \omega_e & 0 \\ -e_x & 2\omega_e \omega_{e_y} - (e_x \times \omega_e)\omega_{e_z} & 2\omega_e \omega_{e_z} + (e_x \times \omega_e)\omega_{e_y} & e_x e'_x \omega_e & 0 \\ 0 & 0 & 0 & 0 & \omega_e \\ 0 & -2e_y \nu'_e \omega_e \omega_{e_y} & -2e_y \nu'_e \omega_e \omega_{e_z} & -e_y \nu'_e \omega_e - 2\omega_e \nu'_e & 0 \end{bmatrix} \quad (47)$$

and $\alpha = [\alpha_1, \dots, \alpha_5]' \in \mathbb{R}^5$.

Notice that all initial conditions of the form $\check{x}_0 := x_0 + \mathcal{N}\alpha$ are indistinguishable from x_0 . Since the initial condition of the beacon is known, that is ${}^B\check{\mathbf{q}}_1(0) = {}^B\mathbf{q}_1(0)$, this implies that $\alpha_1 = \omega_{e_x}\alpha_4$ and $\alpha_2 = \alpha_3 = 0$. Moreover, notice that \check{x}_0 must satisfy the constraints (11)-(13). Imposing the constraint (12) we obtain $\alpha_5 \in \{0, -2\|\omega_e\|^{-2}\omega'_e(\nu_e + {}^B\nu_c(0))\}$. Thus, one solution is $\alpha_5 = 0$, yielding $\alpha_4 = 0$, which is the trivial solution satisfying (11) and (13). The other nonzero solution of α_5 leads to $\alpha_4 = -2\|\omega_e\|^{-2}\omega'_e({}^B\mathbf{p}_0(0) + {}^B\mathbf{q}_1(0))$, satisfying (11) and (13), which is the set defined in (18).

To show the reverse inclusion, consider $z := x_0 + v \in \mathcal{I}_r(x_0)$ where $v \in \text{Kernel}(\mathcal{O}_r)$. Let $r(x(t))$ denote the range output given initial condition x_0 , where $x(t)$ is the solution of (16) with $x(0) = x_0$ and $r(z(t))$ denotes the range output given the initial condition z , where $z(t)$ is the solution of (16) with $x(0) = z$. By noting that $v \in \text{Kernel}(\mathcal{O}_r)$, it follows that $r(z(t)) = C_u(t)\Phi(t, 0)x_0 + C_u(t)\Phi(t, 0)v = r(x(t))$. Since x_0 is an arbitrary point, by definition, system (16) combined with constraints (11)-(13) is weakly observable on $[t_0, t_f]$. The proof for the case of uniform inter-arrival times follows from the later part of Proposition 1. \square

Note that in Theorem 1 we used the fact that $\text{Rank}(\mathcal{O}_{n_r}) = \min(\text{Rank}(\mathcal{O}_r), \text{Rank}(\mathcal{O}_t))$. Thus, the observability condition (17) and the restriction on the inter-arrival times are derived independently from the matrices \mathcal{O}_r and \mathcal{O}_t . This is because the rank of \mathcal{O}_r depends only on ω_e as $\nu_e > 0$ and the rank of \mathcal{O}_t depends only on $t_k \in [t_0, t_f]$ as $\|\omega_e\| > 0$.

Proof. [**Corollary 1**] From Theorem 1 it follows that the set of indistinguishable points is given by (18). Suppose that there is no ocean current or ${}^B\nu_c$ is known. In this case, the set of indistinguishable points is a subset of $\{x_0, \check{x}_0\}$, where \check{x}_0 is a non-trivial point in (18). Let us assume that the point \check{x}_0 is indistinguishable from x_0 . Since ${}^B\check{\nu}_c = {}^B\nu_c$, we conclude that ${}^B\nu_c = {}^B\nu_c - 2\|\omega_e\|^{-2}\omega_e\omega'_e({}^B\nu_c + \nu_e)$, which contradicts with (20). Thus, \check{x}_0 is distinguishable from x_0 and the system is observable. \square

Proof. [**Theorem 2**] Consider the system (16) with initial condition $x_0 \in \mathbb{R}^{12}$. From (2) and (46) we conclude that $e'_z \mathcal{I}_B \mathcal{R}(\eta) = e'_z \mathcal{I}_B \mathcal{R}(\eta_e) \bar{\Phi}_1(t, 0)'$.

Since $S(\omega_e)$ is a skew symmetric matrix it follows that $\bar{\Phi}_1(t, 0)' \bar{\Phi}_1(t, 0) = I, \forall t$. On the other hand, the depth measurements \mathbf{y}_z satisfy $\mathbf{y}_z = C_{u,z} \Phi(t, 0)x_0 = \bar{C}_{u,z} x_0$, where

$$\bar{C}_{u,z} = \left[\begin{array}{ccc|c} -1 & 0 & t & \\ 0 & 1 & 0 & \end{array} \right] \otimes (e'_z \mathcal{I}_B \mathcal{R}(\eta_e)) \quad \mathbf{0}.$$

Note that, $\bar{C}_{u,z}$ is a first order polynomial in t . Thus, each row of the observability matrix corresponding to depth-only measurements system (16) is a linear combination of rows of $\mathcal{O}_z := [I_3 \otimes (e'_z \mathcal{I}_B \mathcal{R}(\eta_e)) \quad \mathbf{0}]$.

Now, the observability of system (16) can be verified by intersecting $\text{Kernel}(\mathcal{O}_r)$ derived in (47) with $\text{Kernel}(\mathcal{O}_z)$. Moreover, since the initial condition of the beacon is known, from Theorem 1 it follows that $\alpha_1 = \omega_{e_x}\alpha_4$ and $\alpha_2 = \alpha_3 = 0$. Intersecting the mentioned null spaces, the following equalities

must hold: $\alpha_4 e'_z \mathcal{I}_B \mathcal{R}(\eta_e) \omega_e = 0$; $\alpha_5 e'_z \mathcal{I}_B \mathcal{R}(\eta_e) \omega_e = 0$. Now, using (15) and noticing that (17) implies that $\psi_e \neq 0$, we conclude that $\alpha_4 = \alpha_5 = 0$. Thus, the intersection of the two null spaces defined above contains only the origin, $\mathcal{I}_{rz}(x_0) = \{x_0\}$, and the system (16) is observable on $[t_0, t_f]$. \square

Proof. [**Theorem 3**] Consider the system (16) with initial condition $x_0 \in \mathbb{R}^{12}$ and let $\omega_e \in \mathbb{R}^3$ be such that (17) does not hold, that is $\omega_{e_y} = \omega_{e_z} = 0$. Moreover, consider that $n_r \geq 3$ measurement samples are available.

We claim that the range-only observability matrix, \mathcal{O}_{n_r} , has rank 3. We show this by using the rank-factorization theorem. Define $\mathcal{O}_r \in \mathbb{R}^{3 \times 12}$ and $\mathcal{O}_t \in \mathbb{R}^{n_r \times 3}$ whose j^{th} row, \mathcal{O}_{t_j} , are given by

$$\mathcal{O}_r = \begin{bmatrix} 0 & 0 & 0 & 0 & 0 & 1 \\ e'_x & e'_x & 0 & 0 & \frac{1}{\nu_e} & 0 \\ 0 & 0 & 2e'_x & \frac{1}{\nu_e} & 0 & 0 \end{bmatrix}, \mathcal{O}_{t_j} := \nu_e \begin{bmatrix} \frac{1}{\nu_e} & -2t_j & t_j^2 \end{bmatrix}.$$

Note that $\text{Rank}(\mathcal{O}_t) = 3$, given $t_k - t_{k-1} > 0$. Moreover, $\text{Rank}(\mathcal{O}_r) = 3$. It can be verified that $\mathcal{O}_{n_r} = \mathcal{O}_t(t_j)\mathcal{O}_r, j \in \{0, 1, \dots, n_r-1\}$ holds, hence by the rank factorization theorem it follows that $\text{Rank}(\mathcal{O}_{n_r}) = 3$. From a standard result in linear algebra, it follows that $\text{Rank}(\mathcal{O}_{n_r}) = \text{Rank}(\mathcal{O}_r)$. This completes the proof of the claim.

Now, using \mathcal{O}_r and \mathcal{O}_z from Theorem 2 it can be verified that the concatenation of the two matrices \mathcal{O}_{rz} has the form

$$\mathcal{O}_{rz} = \begin{bmatrix} [e_y & 0 & 0 & e_y & 0 & 0 & 2e_z & 0 & 0] & [\frac{1}{\nu_e}e_z & \frac{1}{\nu_e}e_y & e_x] \\ I_3 \otimes (e'_z \mathcal{I}_B \mathcal{R}(\eta_e)) & \mathbf{0} \end{bmatrix}.$$

In this case, the null space $\text{Kernel}(\mathcal{O}_{rz}) = \mathcal{N}\alpha$, where

$$\mathcal{N} = \begin{bmatrix} 0 & 0 & \xi_1 & \xi_2 & 0 & 0 \\ \xi_1 & \xi_2 & 0 & 0 & 0 & 0 \\ 0 & 0 & 0 & 0 & \xi_1 & \xi_2 \\ -e_y & 0 & -e_y & 0 & -2e_x & 0 \end{bmatrix},$$

$\xi_1 = e_x + e_z \tan \theta_e / \cos \phi_e$, $\xi_2 = e_y - e_z \tan \phi_e$, and $\alpha = [\alpha_1, \dots, \alpha_6]' \in \mathbb{R}^6$. Imposing the constraint that the initial condition of the beacon is known yields $\alpha_1 = \alpha_2 = 0$. We thus have a 4th order linear subspace and only 3 quadratic state constraints described by (11)-(13). Solving the corresponding quadratic equations we may find a solution for α_4 - α_6 but the fifth order, α_3 , remains as a free parameter. This implies that the set of indistinguishable points is at least a piecewise continuous function of the free parameter α_3 and the system is not weakly observable. \square

Proof. [**Theorem 4**] The proof for the case of range-only measurements is similar to that of Theorem 1 with the only difference that we use the assumption ${}^B\check{\mathbf{p}}_0(0) = {}^B\mathbf{p}_0(0)$. This implies that $\alpha_1 = \alpha_4 = 0$ and $\omega_{e_z}\alpha_2 = \omega_{e_y}\alpha_3$. Moreover, notice that \check{x}_0 must satisfy the constraints (11)-(13). Imposing the constraint (12) we obtain $\alpha_5 \in \{0, -2\|\omega_e\|^{-2}\omega'_e({}^B\nu_c(0) + \nu_e)\}$. Setting $\alpha_5 = 0$ implies $\alpha_2 = \alpha_3 = 0$, which is the trivial solution ensuring that (11) and (13) hold. The other nonzero solution of α_5 leads to

$$[\alpha_2, \alpha_3] = -[\omega_{e_y}, \omega_{e_z}] \|\omega_e\|^{-2} \omega'_e {}^B\mathbf{p}_1(0) / (\omega_{e_y}^2 + \omega_{e_z}^2)$$

ensuring that the constraints (11) and (13) hold. With two possible solutions for α , we conclude that $\mathcal{I}(x_0)$ is given by (21).

Consider now the case where depth measurements are added to the set of observations (similar to the conditions in Theorem 2). The observability of system (16) can be verified by intersecting $\text{Kernel}(\mathcal{O}_r)$ derived in (47) with $\text{Kernel}(\mathcal{O}_z)$, but with the assumption that the initial condition of the AUV is known, meaning $\alpha_1 = \alpha_4 = 0$ and $\omega_{e_z}\alpha_2 = \omega_{e_y}\alpha_3$. Intersecting the mentioned null spaces, the following must hold:

$$(\omega_{e_y}\alpha_2 + \omega_{e_z}\alpha_3) e'_z \mathcal{I}_B \mathcal{R}(\eta_e) \omega_e = 0, \alpha_5 e'_z \mathcal{I}_B \mathcal{R}(\eta_e) \omega_e = 0.$$

At this point, using (15) and noticing that (17) implies that $\psi_e \neq 0$, we conclude that $\alpha_2 = \alpha_3 = \alpha_5 = 0$. Thus, the intersection of the two null spaces defined above contains only the origin, $\mathcal{I}_{rz}(\mathbf{x}_0) = \{\mathbf{x}_0\}$, and the system (16) is observable on $[t_0, t_f]$.

Moreover, using the same reasoning as in Theorem 3, but with the assumption ${}^B\mathbf{p}_0(0) = {}^B\mathbf{p}_0(0)$, we conclude that $\mathcal{I}_{rz}(\mathbf{x}_0)$ is at least a piecewise continuous function of free parameter α_1 . Thus, the system is not observable. \square

Proof. [Theorem 5] For one beacon only, the result follows from Theorems 1-4. Consider now more than one beacon. In this case it can be concluded from (14) that the dynamic equations of each set $\{\mathcal{B}q_i, \chi_i, \chi_{ci}\}$ do not depend on the other sets. This means that the observability of the multiple beacon system can be investigated by analyzing the observability of each single-beacon system and the result follows immediately from Theorems 1-4. \square

REFERENCES

- [1] J. C. Kinsey, R. M. Eustice, and L. L. Whitcomb, "A survey of underwater vehicle navigation: Recent advances and new challenges," in *IFAC Conf. on Manoeuvring and Control of Marine Craft*, 2006.
- [2] A. P. Scherbatyuk, "The AUV positioning using ranges from one transponder LBL," in *MTS/IEEE Conf. on Challenges of Our Changing Global Environment OCEANS '95*, vol. 3, Oct. 1995, pp. 1620–1623.
- [3] M. B. Larsen, "Synthetic long baseline navigation of underwater vehicles," in *MTS/IEEE Conf. and Exhibition OCEANS*, 2000.
- [4] T. Casey and J. Hu, "Underwater vehicle positioning based on time of arrival measurements from a single beacon," in *MTS/IEEE Oceans 2007, Vancouver, BC, Canada*, Sep. 2007, pp. 1–8.
- [5] J. Saude and A. P. Aguiar, "Single beacon acoustic navigation for an AUV in the presence of unknown ocean currents," in *IFAC Conf. on Manoeuvring and Control of Marine Craft*, 2009.
- [6] S. D. McPhail and M. Pebody, "Range-only positioning of a deep-diving autonomous underwater vehicle from a surface ship," *IEEE J. of Oceanic Eng.*, vol. 34, no. 4, pp. 669–677, 2009.
- [7] S. E. Webster, R. M. Eustice, H. Singh, and L. L. Whitcomb, "Advances in single-beacon one-way-travel-time acoustic navigation for underwater vehicles," *The Int. J. of Robotics Research*, vol. 31, no. 8, pp. 935–950, 2012.
- [8] A. Bahr, J. J. Leonard, and M. F. Fallon, "Cooperative localization for autonomous underwater vehicles," *The Int. J. of Robotics Research*, vol. 28, no. 6, pp. 714–728, 2009.
- [9] P. Newman and J. Leonard, "Pure range-only subsea SLAM," in *IEEE Int. Conf. on Robotics and Automation*, Sep. 2003, pp. 1921–1926.
- [10] E. Olson, J. Leonard, and S. Teller, "Robust range-only beacon localization," *IEEE J. of Oceanic Eng.*, vol. 31, no. 4, pp. 949–958, 2006.
- [11] Y. Petillot, F. Maurelli, N. Valeyrie, A. Mallios, P. Ridao, J. Aulinas, and J. Salvi, "Acoustic-based techniques for autonomous underwater vehicle localization," *Proc. of the Inst. of Mechanical Engineers, Part M: J. of Eng. for the Maritime Environment*, vol. 224, no. 4, pp. 293–307, 2010.
- [12] T. L. Song, "Observability of target tracking with range-only measurements," *IEEE J. of Oceanic Eng.*, vol. 24, no. 3, pp. 383–387, Jul. 1999.
- [13] A. S. Gadre and D. J. Stilwell, "Underwater navigation in the presence of unknown currents based on range measurements from a single location," in *American Control Conf. (ACC)*, vol. 2, Jun. 2005, pp. 656–661.
- [14] A. S. Gadre, "Observability analysis in navigation systems with an underwater vehicle application," Ph.D. dissertation, Virginia Polytechnic Institute and State University, 2007.
- [15] P. Batista, C. Silvestre, and P. Oliveira, "Single range aided navigation and source localization: Observability and filter design," *Systems & Control Letters*, vol. 60, no. 8, pp. 665–673, Aug. 2011.
- [16] G. Indiveri and G. Parlange, "Further results on the observability analysis and observer design for single range localization in 3D," *CoRR*, vol. abs/1308.0517, 2013.
- [17] F. Arrichiello, G. Antonelli, A. P. Aguiar, and A. Pascoal, "Observability metric for the relative localization of AUVs based on range and depth measurements: Theory and experiments," in *IEEE/RSJ Int. Conf. on Intelligent Robots and Systems (IROS)*, Sep. 2011, pp. 3166–3171.
- [18] A. P. Aguiar and J. P. Hespanha, "Minimum-energy state estimation for systems with perspective outputs," *IEEE Trans. on Automatic Control*, vol. 51, no. 2, pp. 226–241, Feb. 2006.
- [19] R. Hermann and A. J. Krener, "Nonlinear controllability and observability," *IEEE Trans. on Automatic Control*, vol. 22, no. 5, pp. 728–740, Oct. 1977.
- [20] M. Bayat and A. P. Aguiar, "Underwater localization and mapping: Observability analysis and experimental results," *Industrial Robot: An Int. J.*, vol. 41, issue 2, pp. 213 – 224, 2014.
- [21] A. P. Aguiar and J. P. Hespanha, "Minimum-energy state estimation for systems with perspective outputs and state constraints," in *Proc. 42nd IEEE Conf. on Decision and Control*, Maui, Hawaii, Dec. 2003.
- [22] A. J. Krener and A. Isidori, "Linearization by output injection and nonlinear observers," *Systems & Control Letters*, vol. 3, pp. 47–52, 1983.
- [23] F. Plestan and A. Glumineau, "Linearization by generalized input-output injection," *Systems & Control Letters*, vol. 31, pp. 115–128, 1997.
- [24] H. Nijmeijer and A. van der Schaft, *Nonlinear dynamical control systems*. Springer, Berlin, 1990.
- [25] M. R. Elgersma, "Control of nonlinear systems using partial dynamic inversion," Ph.D. dissertation, University of Minnesota, Minneapolis, USA, 1988.
- [26] N. Crasta, M. Bayat, A. P. Aguiar, and A. M. Pascoal, "Observability analysis of 3D AUV trimming trajectories in the presence of ocean currents using single beacon navigation," in *Proc. of IFAC World Congress*, Cape town, South Africa, 2014.
- [27] R. M. Murray, Z. Li, and S. S. Sastry, *A Mathematical introduction to robotic manipulation*. CRC Press, Florida, 1994.
- [28] A. J. Krener, "The convergence of the minimum energy estimator," in *New Trends in Nonlinear Dynamics and Control and their Applications*, ser. Lecture Notes in Control and Information Science. Springer Berlin Heidelberg, 2003, vol. 295, pp. 187–208.
- [29] D. Simon and T. L. Chia, "Kalman filtering with state equality constraints," *IEEE Trans. on Aerospace and Electronic Systems*, vol. 38, no. 1, pp. 128–136, Jan. 2002.
- [30] S. Boyd and L. Vandenberghe, *Convex optimization*. Cambridge University Press, 2004.
- [31] I. Karafyllis and C. Kravaris, "From continuous-time design to sampled-data design of observers," *IEEE Trans. on Automatic Control*, vol. 54, no. 9, pp. 2169–2174, Sep. 2009.
- [32] V. Hassani, A. P. Aguiar, M. Athans, and A. M. Pascoal, "Multiple model adaptive estimation and model identification using a minimum energy criterion," in *American Control Conf. (ACC)*, Jun. 2009.
- [33] H. K. Khalil, *Nonlinear systems*, 3rd ed. Upper Saddle: Prentice Hall, New jersey, 2007.
- [34] G. Stewart, *Matrix algorithms: Volume 1, Basic decompositions*. SIAM: Society for Industrial and Applied Mathematics, 1998.
- [35] J. Ribeiro, "Motion control of single and multiple autonomous marine vehicles," Master's thesis, Instituto Superior Técnico, Lisbon, Portugal, Nov. 2011.
- [36] A. J. Krener and K. Ide, "Measures of unobservability," in *IEEE Conf. on Decision and Control (CDC)*, 2009, pp. 6401–6406.
- [37] M. Bayat and A. P. Aguiar, "Observability analysis for AUV range-only localization and mapping: Measures of unobservability and experimental results," in *IFAC Conf. on Manoeuvring and Control of Marine Craft*, Arenzano (GE), Italy, 2012.
- [38] J. P. Hespanha, *Linear systems theory*. Princeton: Princeton Press, 2009.



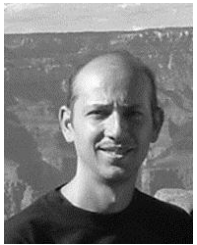
Mohammadreza Bayat received his B.Sc. in Electrical Engineering from the Polytechnic University of Tehran (AUT), in 2004. He completed his M.S. degree in Automation and Instrumentation Engineering from the Petroleum University of Technology, Tehran, in 2007. From 2007 to 2009 he was a researcher at Institute for Systems and Robotics (ISR), Instituto Superior Técnico (IST), University of Lisbon, Portugal. From 2009 onwards he is a Ph.D. student at ISR/IST and being advised by Prof. A. Pedro Aguiar. Currently he is a researcher at

ISR/IST. His main research interest include nonlinear robust/adaptive estimation, data reconciliation, nonlinear observers, underwater robot localization and tracking.



Naveena Crasta received the B.E. degree in Electrical and Electronics Engineering from the Manipal Institute of Technology, Manipal, in 2000, the M.Tech. degree in Control and Automation from the Indian Institute of Technology Delhi, in 2004, and the Ph.D. in Aerospace Engineering from the Indian Institute of Technology Bombay, in 2009. Currently he is a researcher at the Institute for Systems and Robotics, Instituto Superior Técnico, University of Lisbon, Portugal. His research interests include nonlinear systems theory, dynamics and control of

rotational motion, control, navigation, and guidance of autonomous robotic vehicles, nonlinear observers and estimation theory, energy-based control and computational geometry.



A. Pedro Aguiar received the Licenciatura, M.S. and Ph.D. in Electrical and Computer Engineering from Instituto Superior Técnico, University of Lisbon, Portugal in 1994, 1998 and 2002, respectively. Currently, he holds an Associate Professor position with the Department of Electrical and Computer Engineering, Faculty of Engineering, University of Porto. From 2002 to 2005, he was a post-doctoral researcher at the Center for Control, Dynamical-Systems, and Computation at the University of California, Santa Barbara. From 2005 to 2012, he was

a senior researcher with ISR/IST, and an invited assistant professor with the Department of Electrical and Computer Engineering, IST. His research interests include modeling, control, navigation, and guidance of autonomous robotic vehicles, nonlinear control, switched and hybrid systems, tracking, path-following, performance limitations, nonlinear observers, the integration of machine vision with feedback control, networked control, and coordinated/cooperative control of multiple autonomous robotic vehicles.



António M. Pascoal received his PhD in Control Science from the University of Minnesota, Minneapolis, MN, USA in 1987. Associate Professor of Control and Robotics at IST, University of Lisbon, Portugal. Member, Scientific Council of the Institute for Systems and Robotics (ISR), Lisbon. Expertise in Dynamical Systems Theory, Robotics, Navigation, Guidance, and Control of Autonomous Vehicles, and Networked Control and Estimation. Elected Chair, IFAC Technical Committee Marine Systems, 2008-2014. He was IST's responsible scientist for eight

EU funded collaborative research projects and several national research projects, all in the area of dynamical systems and ocean/air robotics. He has cooperated extensively with groups in Europe, US, India, and Korea on the development and at sea testing of robotic systems for ocean exploration. His long-term goal is to contribute to the development of advanced technological systems for ocean exploration and exploitation aimed at bridging the gap between science and technology.